N71-32349

NASA TECHNICAL MEMORANDUM

NASA TM X-67885

NASA TM X-67885

NEW DIRECTIONS IN MATERIALS RESEARCH DICTATED BY STRINGENT FUTURE REQUIREMENTS

by S. S. Manson
Lewis Research Center
Cleveland, Ohio

OPENING LECTURE for presentation at
International Conference on the Mechanical Behavior of Materials
Kyoto, Japan, August 15-20, 1971

NEW DIRECTIONS IN MATERIALS RESEARCH DICTATED BY STRINGENT FUTURE REQUIREMENTS

by S. S. Manson

National Aeronautics and Space Administration
Lewis Research Center
Cleveland, Ohio

SUMMARY

This paper outlines the stringent materials requirements associated with advanced projects such as automotive thermal reactors, jet engines, space shuttle and space nuclear power systems. Illustrations are presented of recent research in each of these areas, emphasizing programs involving either new materials, test techniques, or methods of analysis. Specific results are cited for metal and polymer matrix materials, dispersion strengthening, directional solidification, powder metallurgy, and materials of novel composition. Cryogenic fatigue and fracture, as well as high temperature creep and fatigue are also discussed, with the emphasis placed on new facilities and new analytical techniques that are being developed to treat these problems. The report also emphasizes the concept of technology transport, meaning that materials research, properly documented, provides a baseline for applications often unanticipated when the research was conducted. In fact, the objective of the original research is sometimes not met, but the results of the research pay benefits in terms of other later applications.

INTRODUCTION

This important conference on the mechanical behavior of materials comes at a very appropriate time. The breadth of the subject which is to be covered, the large international participation, and the overwhelming attendance, all attest to both the need for such a conference and to the promise of its contribution to pressing materials problems that lie ahead of us. And indeed, these materials problems are numerous, for many advanced projects in the sea, on land, in the air, and in space, can be successfully accomplished only if suitable materials become available to fulfill the most stringent requirements, and if engineering methods are developed to use these materials in an effective and efficient manner. For example, stringent weight reduction requirements must be met for VTOL and STOL applications; the utmost in material performance and lowest possible cost are the major considerations for a low-cost jet engine and for automotive thermal reactors; reusable thermal protection system materials that can satisfactorily resist the severe heating problems imposed by reentry are a key factor in the space shuttle concept. Applications such as these often require a change in direction in existing materials research areas. In other instances initiation of entirely new research areas is needed. In any case, materials will pace our advanced technology, and we will be able to accomplish only what our materials permit us to accomplish.

It is my pleasant duty to present the opening lecture at this imposing conference A great range of subjects suggest themselves around which the lecture can be structured For almost anything said about mechanical behavior of materials will relate appropriately to some segment of this conference so all-inclusive are its contents I have therefore chosen to divide my talk into two major headings

First I shall try to illustrate some current research in areas pertinent to this Conference limiting myself to contributions that have recently been made at my own laboratory I do this because I am most familiar with our own research and in order not to give the impression that my context is chosen from the field at large thereby avoiding possible offense to investigators whose contributions are not included

Second in order to emphasize the value of conferences of this type I shall formulate some of my illustrations in terms of what might be called a "technology transport" principle By this I mean that technological investigations conducted for one purpose may later find great usefulness in applications not intended at the time of the study The original goals might in fact not have been met, but the results may still be useful elsewhere Conferences of this kind are therefore very valuable in that they put the results on record for whatever later use may arise

In order to carry through this format I shall limit myself to four areas of application 1) Earth-oriented problems 2) aeronautics-

oriented problems, 3) space-oriented problems, and 4) general life prediction methods that are essentially involved in all of these applications.

EARTH-ORIENTED PROBLEMS

General

Let me start first with earth-oriented problems. The question might arise in your minds as to why NASA should be at all concerned with earth-oriented problems. It is, however, very common for NASA to be involved in such problems because we consider the application of space-oriented technology to earth-oriented projects to be one of our vital functions. In carrying out our responsibilities in this regard, it is often necessary to have direct participation of our scientists and engineers on research programs affiliated with other public and private institutions. Therefore, wherever possible, and especially if it can be done with a minimum of cost and effort, we try to contribute our facilities and expertise to the solution of problems relating to the public welfare.

For example, we have made contributions in health and in biomechanics problems. As an illustration of an earth-oriented contribution in the field of health, I might cite work that we have recently done in connection with the role of trace metals in nutrition. We have at

laboratory a very advanced spectrographic method that was developed for the rapid determination of the constituents of materials (ref. 1). The technique can detect 1 billionth of a gram (10^{-9} gram) of most metals and can be applied to samples weighing as little as a few micrograms. Our primary interest was the rapid determination of the elemental content of a wide variety of alloys without the need of a standard sample. Because of its sensitivity, the technique is useful in determining parts per billion (ppb) of trace impurities. We have found that such minute contents can have large effects on mechanical behavior of certain alloys. In nutrition, too, it has been found that a few ppb of some metals can have large effects. For example, at the University of Colorado Medical School at Denver, a research physician was interested in measuring trace element content in the range of several ppb in human body fluids in order to define efficiency levels for various metals, primarily chromium in relation to diabetes. He contacted our Mr. William Gordon, who had developed the sensitive spectrographic technique, and enlisted his participation. The method is now being used routinely to monitor levels of chromium and other metals in clinical patients.

Biology and biomechanics are areas within the scope of the NASA charter because of the importance of these subjects in man's performance in space. Other NASA Centers are much more intimately involved in these subjects than we are, but we also are contributing. Some of our contributions are outgrowths of our materials research efforts.

For example, the Cleveland Clinic recently learned of our ultrasonic facility which was being used to study liquid metal cavitation. A research physician at the Clinic became interested in the use of ultrasonics in treating eye cataracts and asked for our assistance. With relatively little effort, we were able to help him. His research is still continuing and hopefully we shall all benefit from his findings. We have also assisted medical people in the study of the mechanical aspects of artificial heart valves and other components of the human body.

Ecology and pollution have recently become very common words. Obviously NASA is concerned with gas pollution and noise pollution of aircraft. Because of the expertise of our staff in problems of combustion and metal usage, we have been asked by other Government agencies to assist in the solution of other pollution problems as well. One such effort we are making is to assist the City of Cleveland in mapping the presence and origin of various toxic metals in the environment. In another program, we are assisting the Environmental Protection Agency to obtain a solution to automotive exhaust problems. I shall later discuss this effort in detail.

Regarding ecology, it is well known that NASA is preparing an EARTH RESOURCES TECHNOLOGY SATELLITE (ERTS-A to be launched in 1972 and ERTS-B in 1973). This satellite will be used to make earth observations which can help in ecological matters. Being located, as we are, in the Great Lakes area, we are concerned with the growth of algae in Lake Erie.

We feel that satellites will permit observations of color gradations that are very revealing of the state of marine life in our locality. Several members of our staff are participating in the development of a remote rapid evaluation system for detecting color gradations. The system may help us in evaluating methods for slowing down the eutrophication of our lake.

We have also made serious attempts to contribute to the regional commerce of our area. For example, the strategic location of the Great Lakes is such that it serves a geographical area which produces 43% of our gross national product. Much of this product could possible be shipped by way of these Lakes. Yet this large inland body of water is currently used only 8 months of the year because of ice hazards. If we had a better understanding of the origin of the ice and the types of ice involved, we might be able to determine optimum ice-breaking routes and thereby extend the shipping season, eventually to the entire year. The EARTH RESOUCES SATELLITE, hopefully, will provide us with much useful information to help achieve this goal. Recently we have also participated in the design of a large jetport that might be located in Lake Erie as a means of extending air transportation to Cleveland to the large surrounding geographical area.

The Automotive Thermal Reactor

I shall now elaborate on a specific earth-oriented materials program we are conducting in order to assist the Environmental Protection

Agency. All of us are concerned with the exhaust that comes out of automobiles, and how it pollutes the environment. We well know that if the combustion could be carried to a greater degree of completion there would be fewer pollutants in the exhaust gas. One of the ways in which we are attempting to combat this problem, therefore, is to provide an afterburner (thermal reactor) to replace the exhaust manifold. Here the exhaust gases can be burned more completely, reducing the products of combustion to a less noxious form. Many problems are involved in this approach, relating largely to high temperatures developed when the combustion is carried to a higher degree of completion.

Our work in this area is being done under the leadership of Neal Saunders and Charles Blankenship (ref. 2). Figure 1 shows a schematic diagram of a thermal reactor we are studying. It replaces the exhaust manifold and serves as a combustion chamber where gases such as CO are further burned to produce CO_2. The added burning, of course results in high metal temperatures. Table I outlines some of the requirements and problems involved.

TABLE I - FACTORS AFFECTING MATERIALS SELECTION FOR AUTOMOBILE THERMAL REACTORS

HIGH COMBUSTION TEMPERATURE
870° to 1040°C (1600° to 1900°F) in ordinary operation
1260°C (2300°F) under spark-out conditions
LONG CYCLIC LIFETIME
50,000 to 100,000 mile life
10,000 to 20,000 engine on-off cycles
SEVERE CORROSION AND EROSION CONDITIONS
High temperature oxidation
Erosion from exhaust gas particulates
Chemical attack from fuel constituents
LOW COST
Less than $50 for assembly
Easy fabrication and assembly
Use of relatively available materials

As can be seen in Table I, temperatures in the neighborhood of 870° to 1040°C (1600° to 1900°F) are developed under normal driving conditions, and temperatures as high as 1260°C (2300°F) must be withstood for short periods during emergency. The unit must be able to survive between 50,000 to 100,000 miles of life, including, of course, the thermal fatigue associated with starting and stopping. The very high temperatures involved result in oxidation of the reactor material, erosion from the exhaust gas particulates, and chemical attack from the fuel constituents. Superimposed on the mechanical and metallurgical problems are the requirements that the reactors be of low cost, be relatively easy to fabricate and assemble, and not require strategic materials that could become unavailable when multi-million units are built each year. Figure 2 shows some of the results we have obtained to date in

an engine program we are conducting (ref. 3) in cooperation with the Environmental Protection Agency. Full size reactors fabricated from several candidate materials are being evaluated. In the upper part of the figure we see the temperature variation for several service functions and the test cycle that is being used in the study to evaluate the performance of reactor materials. In the lower half of the figure is shown the weight loss of full size reactor cores as a function of exposure time. Note that the AISI 310 stainless steel and coated AISI 651 stainless steel are not satisfactory because of large weight losses in very short periods of time. The most promising alloys in our study, Inconel 601 and GE 1541, exhibited excellent oxidation resistance through 600 hours of exposure. Inconel 601 is a nickel base alloy, and might present a problem for reactor use because of the limited availability of nickel when considering large material quantities associated with multi-million unit requirements. The GE 1541 alloy, on the other hand, is an iron base alloy containing only 15 percent chromium, 4 percent aluminum, and about 1/2 percent yttrium. It should not be inferred, of course, that either of these alloys is the final successful candidate. In fact, we are studying many different approaches to the problem. For example, we are looking at other alloys and coatings as well as the use of non-metallic materials for this application. At this time the data in figure 2 suggest only that there are potential candidate materials which may be used successfully in a thermal reactor,

but no final conclusions can be reached until the study is complete.

Figure 2 also enables me to provide my first illustration of the technology transport principle mentioned earlier. The GE 1541 alloy was not developed originally for this application at all. It was developed by the General Electric Company under contract with the Atomic Energy Commission for an altogether different application. What was needed was a ferritic alloy capable of resisting a steam environment, and this alloy resulted. It was never applied extensively for the purpose for which it was developed, however, because of a change in direction of the program with which it was connected. When the automotive thermal reactor application arose, the material was available for possible use. The value of the research invested in the material was conserved. It might be mentioned that the small content of yttrium included in the alloy to promote oxide adherence, may not be a necessary ingredient for the automotive application. We are studying this matter further. In any case, we are heirs to a material developed for one purpose, but of potential usefulness in an altogether different application.

AERONAUTICS-ORIENTED PROBLEMS

The provision of suitable materials for aeronautics application is not new, but it remains of utmost importance despite the many

years of research effort in this area. Among the materials problems are those concerned with VTOL and STOL applications, the provision of a low cost jet engine, and the achievement of a quiet engine.

To illustrate aeronautics problems in which we are currently engaged, I shall draw on materials research recently conducted for jet engine applications, specifically composite compressor blades, intermediate and high temperature alloys for disks and turbine blading, and problems associated with oxidation and corrosion of the materials used in the high temperature portions of the engine.

A jet engine is a heat engine, and the higher the working temperature the higher is the efficiency and specific output. For example, a 200°C increase in the inlet gas temperature to the turbine of a jet engine can result in an increase in specific thrust of the order of 30 percent for a constant value of specific fuel consumption. Therefore, we seek the highest temperatures possible. And high turbine inlet gas temperatures, together with high airplane velocity mean higher temperature throughout the entire engine.

Composite Compressor Blades

Compressor blades are large, they must be rigid, they must sustain moderately high temperatures, and they must be light because of centrifugal loading, and airborne service. Some work has already been conducted on composite blades, using metallic and non-metallic

fibers and matrices. To date the most advanced composites have involved epoxy resin matrix materials. But these composites are only capable of withstanding continuous use temperatures of about 149°C (300°F). Higher temperatures, of the order of 260°C (500°F) or 316°C (600°F) are desired, but to accomplish this goal advanced research is needed. Several different types of high temperature resistant resins are possible (ref. 4), among them a class described as "condensation" type polyimides. These can sustain high temperatures, but involve some problems, as derived from the characteristics shown in Table II.

TABLE II - CHARACTERISTICS OF POLYIMIDE RESINS

	Condensation Type	Addition Type (Prepolymer)	Addition Type (Monomer)
Solvent Requirements	High Boiling Polar Solvent, Toxic	High Boiling, Polar Solvent, Toxic	Low Boiling Alcohols Nontoxic
Solubility, (Solids Content, %)	20 - 40	20 - 40	60 - 70
Viscosity	Medium to High	Medium	Low
Solution Stability	Good	Fair to Poor	Excellent
Processability	Very Poor	Excellent	Excellent

The condensation type polyimide, because of its large chain-length construction, requires a large quantity of high boiling solvent,

which is also toxic. The requirement to remove the solvent, and the water released during imidization results in porosity that is detrimental to mechanical properties of the composite (ref. 5). During evaporation of the solvent some premature formation of the thermally stable imide rings can occur converting the polymer into an infusible condition. Further removal of volatiles and consolidation during final processing is extremely difficult - resulting in high porosity, as much as 10-15%. In addition, high viscosity prevents good wetting of the fibers by impeding fluid flow into the interstices of the very fine fibers during impregnation.

The addition-type polyimides avoid many of the problems associated with the condensation types, as may be seen from Table II. Two classes have been studied - the intermediate chain-length prepolymer type, and the very small chain (essentially) monomer type. Both show great improvement over the condensation type, especially so the monomer variety, which avoids toxicity and low solubility problems, and has low viscosity and excellent processibility (ref. 6). It is also extremely stable in solution, which is reflected in good shelf life, compared to the prepolymer type.

At this point I can again invoke our technology transport principle. The polymer we have recently studied with considerable success is designated PIOP. It was originally developed by TRW, under contract to NASA, when our interest was in ablative materials, for possible use in rocket exhaust nozzles. It was not an outstanding

material for this purpose, but its characteristics were documented and the material was set aside for later use. Interest revived when we needed a high temperature laminating plastic, for which purpose it proved to be very useful. Most of our research was conducted on the TRW prepolymer material, but the monomer variety was later introduced by T. T. Serafini and his associates at our Center in order to overcome the limitations of the prepolymer discussed above and outlined in Table II.

Figure 3 shows some test results with a composite made from the prepolymer variety PIOP (using the graphite Fortafil 5Y as a reinforcing fiber). The flexural strength is plotted as a function of exposure time for temperatures of 260 and 316°C (500 and 600°F). At 260°C (500°F), there is actually a small increase in strength during exposure (due probably to additional curing), and high strength is maintained for at least 1000 hours (end of test). At 316°C (600°F), the higher strength is reached almost immediately, but the strength decreases with exposure time. About 80 percent of its strength is retained for about 400 hours; therefore, the material is suitable principally for short bursts of power to temperatures as high as 316°C (600°F). Since the epoxies, which are the commonly used plastics today, are limited to temperatures of about 149°C (300°F), it is seen that the PIOP system represents a significant advance over the state-of-the-art.

Most of our early work in PIOP was done on the prepolymer form, Fig. 3, for example. In our later work the monomer was introduced

because of its advantages. To determine whether the use of monomeric reactants resulted in composites having inferior properties, a series of duplicate tests was conducted using both forms. The results are shown in Figure 4, which shows weight loss and interlaminar shear data for these materials. It is seen that the properties are the same whether the monomer or prepolymer is used. Thus, because of the advantages of the monomer approach outlined in Table II, our future work will be concentrated on the monomeric reactants.

Materials for the Intermediate Temperature Range

The intermediate temperature range in the vicinity of 649°C (1200°F) is of special interest in the gas turbine engine because this is an important operating temperature range for the turbine disk. A need exists for stronger fabricable materials for this application. One approach we have followed involves the use of pre-alloyed powder metallurgy.

First, let me outline the process for preparing the prealloyed powder material. A schematic diagram is shown in Figure 5. The raw materials for the alloy are vacuum melted. When the melt is poured the molten metal is atomized by means of inert gas jets. The rapid cooling rate of the atomized metal droplets produces a very fine powder that is very uniform in composition. This powder

is then collected, sized, and consolidated by extrusion or hot-pressing and can then be subjected to any desired heat treatment The important characteristics of this material are:

a) its very fine grain size which promotes high strength at room temperature and in the intermediate temperature range

b) uniformity of the microconstituents, in contrast to coarse segregations associated with cast ingots Maximum usage of the alloying constituents is thus accomplished, again promoting strength

Some results that have been obtained by J. C. Freche and his co-workers at our laboratory are shown in Figure 6. The alloy is TAZ-8A, which is a nickel base material, containing a number of alloying constituents including tantalum, aluminum and zirconium (ref. 7) Note that for temperatures up to 649°C (1200°F), the extruded powder product is nearly twice as strong as the as-cast material of the same composition (ref. 8). At temperatures above 760°C (1400°F), the as-cast material is stronger, however, because coarse grains (small grain boundary surface area) promote strength in the high temperature range where the grain boundaries are weak. Note also from Figure 6 that extremely high tensile elongations can be obtained at temperatures above 927°C (1700°F). The significance of this "super-plasticity" can be seen in Figure 7 where a 2.54 cm (1-inch) test specimen is seen to have been extended to a length greater than 15.2 cm (6 inches) after test at 1038°C (1900°F).

Figure 8 dramatically demonstrates the potential practical utility of the superplastic characteristics of prealloyed powder products. Shown here is a powder metallurgy TAZ-8A turbine blade which was forged in a die made from the same TAZ-8A alloy. However, the die was a cast product, and thus did not deform while pressing the powder material to shape. The opportunities for inexpensive and precise forming of powder metallurgy parts are, of course, very enticing.

A further example of the usefulness of the prealloyed powder approach is shown in Figure 9 (ref. 9). Here the alloy is VI-A, also nickel base, with numerous alloying additions. It was developed jointly by NASA and TRW. Conventional wrought alloys are inherently limited in alloying content because of segregation and because of the difficulty in deforming very strong, highly alloyed materials. Prealloyed powder techniques afford us the opportunity to form highly alloyed materials. Since VI-A has a high alloy content it is extremely strong at high temperatures; it was therefore of interest to us to determine if it could be used as a basis for a stronger intermediate temperature alloy than current wrought products. As shown in Figure 9, a strength of 1620 MN/m^2 (235 ksi) was achieved at 649°C (1200°F), which is a 43 percent increase in strength over the cast alloy at this temperature, and to our knowledge a substantial increase over the strongest wrought alloy at 649°C (1200°F) in use today. Note also that superplasticity was developed in this alloy at 1093°C (2000°F). We are pursuing our studies with this alloy to determine methods of

of increasing the strength of prealloyed powder products at high temperatures, thus taking full advantage of the segregation-free structures obtained in this way.

Materials for the High Temperature Range

The temperature range above 927 to 982°C (1700 to 1800°F) is of great interest to us for turbine stator vanes and for the turbine blades of early stages of advanced engines. We are pursuing several approaches, which I shall now outline.

Compositional variations - It is natural to look to the refractory metals, because of their higher melting point, as a basis for alloys suitable in the high temperature range. We are, indeed, working on chromium, molybdenum, and tungsten base alloys. Needless to say, such alloys encounter problems of oxidation and embrittlement. Time limitations do not permit me to discuss recent progress in detail. I shall limit my remarks to our work on WAZ-20 (ref. 10), another nickel-base alloy developed by Freche and his co-workers, which contains large additions of tungsten to improve refractoriness and strength at high temperature. The composition of the alloy is shown in Table III.

TABLE III - NOMINAL COMPOSITION OF WAZ-20
(in weight percent)

W	Al	Zr	C	Ni
17 - 20	6 - 7	1.4 - 1.6	0.10 - 0.20	Bal

TABLE IV - INCIPIENT MELTING POINTS OF NICKEL BASE ALLOYS

Alloy	°C	°F
B-1900	1204	2200
MAR-M200	1204	2200
IN-100	1210	2210
VI-A	1246	2275
NASA WAZ-20	1302	2375

The composition shown in Table III was carefully chosen to avoid the possibility of low-melting-temperature phases. Note especially how few are the alloying additions, in contrast to commonly used nickel base alloys which contain as many as 8 to 10 alloying elements. That refractoriness is achieved is seen in Table IV which compares the incipient melting points of other commonly used alloys to that of WAZ-20. Incipient melting of the latter alloy is raised by at least 55°C (100°F) beyond that of any of the other alloys shown.

Figure 10 shows a comparison of the tensile strength of WAZ-20 and several other representative cast nickel-base alloys at 1204°C (2200°F). It is more than twice as strong as our TAZ alloys and B-1900, and at least 50 percent stronger than TD-Nickel, a dispersion strengthened powder metallurgy product which is reputed for its high temperature strength.

Directional solidification - Because of the weakness of grain boundaries at high temperature, it is natural to seek materials containing a minimum of such boundaries, particularly those located

transverse to the applied loading. Material which is solidified from the melt in a controlled fashion so as to avoid the presence of transverse grain boundaries has proven to be very advantageous for high temperature applications for reasons of strength, ductility, and low elastic modulus. All these factors, for example, enhance thermal fatigue resistance. The early work on directionally solidified alloys for jet engine use was performed at Pratt and Whitney Aircraft Company largely with the nickel base alloy MAR-M200. We have been particularly interested in the application of the technique to the alloys developed by Freche and his co-workers. Figure 11 shows the grain structure of tensile specimens of the conventionally cast and directionally solidified WAZ-20 alloy previously discussed, and figure 12 shows the creep rupture behavior of these two forms of the alloy when tested (ref. 10) at a stress of 103 MN/m^2 (15 ksi). Plotted is the rupture time versus the test temperature. It can be seen that at a given temperature the rupture time is approximately doubled by directional solidification, or for a selected rupture time the permissible temperature is raised approximately 28°C (50°F) by directional solidification. We have also found that directional solidification substantially enhances thermal fatigue resistance and that this indeed may be one of its greatest advantages insofar as turbine blade applications are concerned.

Dispersion strengthening - The incorporation of a fine stable dispersoid in a metallic matrix is a very promising way of achieving

high temperature strength. Work on dispersion-strengthened materials has been conducted for many years at our Laboratory by J. W. Weeton, M. Quatinetz and their co-workers. In our approach, the dispersion is accomplished by mechanical intermixing of fine powders of matrices and dispersoids (references 11 to 14). This is in contrast to some commercial processes (such as those whereby TD-Nickel and TD-Nickel Chromium are produced) which are basically accomplished by a chemical-colloidal approach. We feel that our process, which we designate NASCAB (standing for NASA Method of Comminution and Blending) lends itself more readily than chemical-colloidal methods to the pairing of matrices and dispersoids of arbitrary selection, thus giving us more freedom to optimize the choices.

A schematic diagram of the process is shown in figure 13. Both the matrix material and dispersoid may be ground together or separately to submicron size. In either case they are thoroughly intermixed and compacted into thin slabs. During sintering of nickel and nickel-chromium matrix slabs, copious quantities of hydrogen are provided to insure removal of matrix-impurity oxides. Heating is provided at a carefully controlled rate to reduce the oxides and remove moisture in a way that avoids the detrimental effects of the moisture effluent. After the slabs have been sintered to a density of approximately 80%, final consolidation is accomplished by alternately rolling and annealing treatments which produce a microstructure on which the inherent strength of a dispersion-strengthened

material depends. If large bodies are required a number of the small slabs may be consolidated by hot pressing prior to the rolling.

The importance of using small slabs providing hydrogen cleaning, and controlled-rate heating - as reflected in the microstructure of the material - is shown in figure 14. When the precautions are not used the particles agglomerate into coarse groups as shown by the microstructures on the left and the material does not display the desirable fine dispersoid structure shown at the right of the figure The latter was accomplished when all of the innovations outlined (references 13 and 14) were introduced. Both specimens shown in figure 14 were annealed at successively increasing temperatures up to 1430°C (2600°F).

Figure 15 shows some experimental results of tensile tests at 1093°C (2000°F) of dispersion strengthened sheet versus number of cold-roll anneal cycles It is seen that the NASCAB process is capable of producing considerably higher strengths than the conventionally used processes for TD-Ni and TD-NiCr. With a 4% dispersoid of thoria in nickel, readily obtainable by this process a remarkably high tensile strength of 165.6 MN/m^2 (24 ksi) can be achieved Figure 16 shows some results of the 100-hour creep rupture strength for the 4% - thoria NASCAB material. A stress level of approximately 82.8 MN/m^2 (12 ksi) can be supported for 100 hours at 1093°C (2000°F) with the NASCAB sheet compared to much lower levels for TD Ni (48.4 MN/m^2 (7 ksi)) and TD-NiCr (41.3 MN/m^2 (6 ks

Fiber reinforced composites - I have already discussed the use of fiber-reinforced composites in connection with compressor blading applications, using polymer matrices. For use at much higher temperatures we must resort to a metallic matrix material. Work on metallic composites was initiated at our Laboratory about fifteen years ago by J. W. Weeton and R. A. Signorelli, and their co-workers. At first we concentrated on model systems (ref. 15) using copper as a matrix and tungsten filaments as reinforcement. These materials do not interact metallurgically, and therefore lend themselves ideally to fundamental studies of the laws that govern composite behavior in the absence of metallurgical interaction. Figure 17 shows an enlargement of the cross-section of a bar of such a composite. Later, as we started to consider matrix materials more suitable for high temperature applications, we learned of the importance of metallurgical interaction (references 16 and 17). Figure 18 shows what can happen when metallurgically incompatible matrix and reinforcement materials are involved. When only 10% nickel was added to the copper matrix attack occurred in the surface regions of the tungsten fibers during 1 hour exposure of the liquid matrix at about 1204°C (2200°F). For a nickel matrix in the liquid state, the disintegration was complete, as shown in the figure.

From later studies we learned several cardinal principles (refs. 18 and 19) regarding the preparation of high temperature metal-matrix composites. The fiber diameters should be sufficiently large to provide an adequate load-carrying core area even if some attack occurs on the

surface; the matrix material composition should be specially selected to minimize interaction with the fiber; and solid-state sintering is preferable to liquid-state infiltration in order to reduce temperatures and interactions.

Results of some recent research on metal matrix composites with possible suitability for high temperature use are shown in figures 19 and 20 (unpublished data from D. W. Petrasek). Figure 19 shows the ratio of stress-to-density for 100 hour life at 1093°C (2000°F) for several fibers of interest to us. Values are shown for a tungsten-2 v/o ThO_2 fiber which has been utilized in a past investigation (ref. 18), and several new fibers. The fibers in one case were of B-88*, and in another a tungsten-hafnium-carbon alloy recently developed at our Laboratory. Compared to conventional superalloys these fibers show strength-to-density values four to five times as high. In Figure 20 are shown results for composites made from these fibers when incorporated in a nickel-base alloy matrix. The nickel-base alloy was preselected to be compatible with tungsten base fibers. Work has already been completed using W-2ThO_2 fibers in the nickel-base alloy described. Composites with fiber contents as high as 70% were produced (ref. 19). For this composite, the 100-hour stress-rupture strength-to-density at 1093°C (2000°F) is about twice the value achievable by conventional alloys shown in Figure 19. Work is progressing on the B-88 and tungsten-hafnium-carbon reinforced alloys, but the research is not yet complete. The bar graphs show our estimates based on fiber properties of what we

*(Cb-28W-2Hf-.07C)

believe can be achieved with composites in the near future. The 70 volume percent W-Hf-C fiber composite would appear to have the greatest potential.

Here again it is perhaps possible to emphasize our technology transport principle. The tungsten-hafnium-carbide material was developed at our Laboratory with altogether different applications in mind from that of fibers in composites. We were interested in extremely refractory materials at the time, and reasoned that combining the highest melting point metal (tungsten) with the highest melting point compound (HfC) would advance our purpose. The product is indeed strong at extremely high temperatures, but its application in connection with matrix reinforcement at 1093°C (2000°F) described here is at a much lower temperature than that originally conceived for use of this material. Nor was the material originally intended for use as a fiber; it was developed for use as a bulk material. That it is proving more interesting as a fiber for use at a much lower temperature range than originally conceived is proof that we do not always know what fruits our research will bear. We must document our results and permit the future to write its own chapter on the value of our research.

Oxidation and Corrosion Problems

The subjects of oxidation and corrosion have commanded our attention to an ever-increasing extent in recent years. It is a subject of special interest in high temperature engines. As can be seen in Figure 21 (ref. 20), several curves are plotted against calendar year of

occurrence. The straight line through the circled data points shows the trend in increasing temperature capability (using as a standard the temperature for which the creep rupture time is 1000 hours at 20 ksi). The circled points show the year in which each alloy was introduced. Progressive increases in strength have been accomplished usually by the addition of a complex array of alloying elements, and, generally, by the reduction of chromium content. The trend in reduction of chromium is also shown in the figure. With decreasing chromium has, of course, come a decrease in resistance to corrosion and oxidation, since it is chromium oxide that provides major protection against environmental attack. Thus, the shaded band is shown, depicting the limiting temperature based on corrosion.

In the late 1940's and in the 1950's temperature limitations based on strength were lower than those based on corrosion resistance, and major research programs were directed primarily at increasing strength potential. In recent years, however, the corrosion limit has become lower than the strength limit. It is appropriate, therefore, to array a major program against the corrosion problem, which is being conducted at our Laboratory under the leadership of H. B. Probst (whose main objective is to study the mechanisms involved) and S. J. Grisaffe (whose main area is the study of protection by coatings and claddings).

The problems of corrosion, are of course, very complex. Table V (ref. 20) shows some of the factors that complicate the mechanism. The presence of mechanical abrasives, chemically reactive species,

extreme temperatures and pressures (which broadens the range wherein salts can remain molten and reactive), and of cyclic conditions of stress and temperature which cause spalling, are but a few of the factors that complicate the mechanism. In addition, complex chemical and metallurgical processes take place, often difficult to predict. Our approach has, therefore, been both experimental and analytical.

TABLE V - CORROSION IN GAS TURBINE ENGINE

Condition	Result
Oxidizing Gas Combustion Products S_2, V, Salt, H_2O	Accelerated Corrosion
Cyclic Temperature and Stress	Spalling, Thermal Fatigue
High Gas Velocity Sand and Carbon particles	Erosion and Vaporization
High Pressure	Condensed Salts

Figure 22 shows some results that emphasize the nature of the problem. Here we show the weight change as a function of exposure time for the nickel base alloy, IN-100, and the dispersion strengthened material, TD-NiCr. Under the static conditions of a laboratory furnace the weight change is slight and consists of a minor increase due to oxidation. Although both materials perform well under the static furnace condition, the TD-NiCr shows even less weight gain than the IN-100. In a high velocity gas burner, however, where erosion and/or vaporization quickly remove the protective scale that forms, both

metals show rapid loss in weight, and TD NiCr loses weight more than four times as rapidly as IN 100. These results show the danger of attempting to rate materials for oxidation resistance from static furnace tests if the real service conditions involve high velocity gas flow.

That the problem is compounded by thermal cycling is demonstrated in Figure 23 (refs. 20 and 21). Here the results are for a cobalt base alloy, WI-52. In a static isothermal furnace the alloy displays weight gain due to oxidation. If the furnace is shut down once every twenty hours -- causing the material to spall as a result of the thermal stresses introduced -- there is a weight loss after 50 hours. If the furnace is shut down in one-hour cycles substantial weight loss develops as a result of the larger number of thermal cycles. The oxidation mechanism of WI-52 is metallurgically extremely complex. C. E. Lowell and I. L. Drell at our Laboratory, have made an extensive study of the process (refs. 22 and 23) and have provided interesting conclusions, many of which have a bearing on the oxidation of other superalloys.

One of the materials we are currently studying intensively is TD-NiCr. Interest in this alloy stems from its potential application in advanced gas turbine engines as well as in the space shuttle, which I shall discuss later. The material containing 20% Cr, was developed as an improvement over TD-Ni from the standpoint of oxidation resistance and room temperature strength. However, we found that while the

material has excellent oxidation resistance under static furnace conditions, high gas velocity is very detrimental to its oxidation resistance (ref. 24). The problem is illustrated in Figure 24. Here the test conditions were more pertinent to those to be encountered in the space shuttle application than in a gas turbine, but the basic problem is the same, so I shall discuss it here instead of later. In Figure 24(a) we see that after exposure for 50 half hour cycles to high velocity gas at 1204°C (2200°F) and 15 Torr pressure, the interior of the sheet developed high porosity. The tests were conducted at the Ames Research Center of the NASA (ref. 25), but it was our responsibility to determine the cause of the behavior, and to suggest remedial measures. Our studies revealed that the porosity was due to the loss of chromium from the alloy. This loss is associated with the vaporization of the normally protective Cr_2O_3 surface scale. The overall mechanism is somewhat complex (ref. 24); however, it is apparent that the loss is greatly accelerated in a high velocity gas stream. The problem becomes acute in both the space shuttle and in the gas turbine engine.

Figure 24(b) shows one solution to the problem. By adding a proper amount of aluminum to the alloy one can cause the formation of a surface aluminum oxide which is far more resistant to vaporization than Cr_2O_3. A small addition of yttrium is believed to enhance the adherence of the aluminum oxide scale. Thus, the TD-NiCrAlY material shows no porosity after 40 cycles of heating, whereas 50 cycles caused large porosity in TD-NiCr.

Figure 25 (ref. 26) shows an alternate approach involving the same basic principle. Here, instead of making the entire sheet from material containing aluminum, a cladding of aluminum - containing material is bonded to the surface of the regular TD-NiCr. The test conditions simulate those occurring in a jet engine, and it is seen that the cladding substantially increases the life of the TD-NiCr substrate material (ref. 26). In this case no yttrium was used in the cladding. Our tests here are in their early stages, but we plan to pursue these promising results.

Once again, I can refer to our technology transport principle. The concept of adding aluminum to TD-NiCr first arose in connection with jet engine applications. When the problem arose in connection with the space shuttle application, directions toward solution were already established. Furthermore, funding for space shuttle development was much more adequate than for jet engine application. So the problem could be vigorously attacked in this connection. Whether alloys such as TD-NiCrAlY will ever be used in the shuttle is not known as yet; many contending designs and materials are being examined, and which will emerge the victor is yet to be determined. But whatever the future for TD-NiCrAlY in the space shuttle, the research on this material will be useful for the jet engine and very likely for other applications as well. Disseminated research results usually find a pay-off.

SPACE-ORIENTED PROBLEMS

Let us turn next to space-oriented problems. While numerous other selections could be made, I shall limit my remarks to the space shuttle and to space nuclear power, both of which are commanding an appreciable amount of attention from us at the present time.

Space Shuttle

The space shuttle is NASA's latest concept for reducing the cost of space flight. Instead of sacrificing the costly boost vehicle in every space shot, as is currently done, the intent is to provide a reusable system, good for about 100 missions. Many different concepts are now being evaluated, and the final design has not yet emerged. However, there are many basic materials problems that require attention so that the final decisions will be wise ones. I shall discuss some of them.

To provide a "feel" for the type of system we are discussing, I have shown in Figure 26 a schematic diagram of the shuttle as presently envisioned. It will consist of two stages - a booster that will transport both itself and an orbiter into space, and the orbiter which will be fired from the booster once the system is in space. The booster then returns to earth; the orbiter also returns to earth later, after it has fulfilled its mission. Although design studies have not been completed, the size and weight approximations shown in Figure 26 are realistic, and very impressive when compared with aircraft of general familiarity.

The thrust system of the booster will undoubtedly involve the storage of pressurized cryogens - very likely oxygen and hydrogen, as our Saturn system used for the Apollo program. Because of multiple re-use requirements, we must be concerned with potential cryogenic fatigue problems. Also, because of efficiency requirements for the large tank sizes involved, cryogenic fracture control is a very important consideration. Eventual re-entry into the earth's atmosphere will involve high surface temperatures, hence the need for a reusable thermal protection system. I shall, therefore, illustrate some recent research we have conducted regarding cryogenic fatigue, cryogenic fracture control, and materials development for reusable thermal protection systems.

Cryogenic fatigue - To be able to perform research on cryogenic fatigue problems, particularly involving the hazards of liquid hydrogen, it has been necessary to develop a special cryostat, sectional view of which is shown in Figure 27. Many materials have been tested to date to determine their relative merits in cryogenic fatigue and to study if the basic mechanism of fatigue at cryogenic conditions is different from fatigue at room temperature. Much of our work has been done under liquid nitrogen and liquid helium environments because the temperatures associated with these cryogens are very close to those of oxygen and hydrogen respectively, while avoiding the hazards associated with these latter fluids.

One of our first efforts in this program was to determine if the basic relations we have developed for fatigue behavior at room

temperature would be valid at cryogenic temperatures as well. The "universal slopes equation", which I suggested a number of years ago (ref. 27) for estimating cyclic life at a given strain range from a knowledge of only tensile properties (ultimate tensile strength, ductility, and elastic modulus) provided a natural framework around which to base our analysis. Figure 28 shows typical results for a titanium alloy. Shown are two straight lines, A and B, computed using the equations listed in the figure, and a curved line C derived by linear addition of lines A and B at each value of cyclic life, N_f. The data points show the experimental values obtained for this material in liquid helium, and are seen to agree well with the predicted lines. Figure 29 shows a summary of results for a number of alloys tested in both liquid nitrogen and liquid helium (ref. 28). The plot is similar to the one used when the universal slopes equation was first proposed, and shows measured life against life predicted from the imposed strain range and cryogenic tensile properties. A 45° line represents perfect correlation, and it is seen that the data points range reasonably around the 45° line. For reference, the dots are a reproduction of the corresponding correlation made on a number of materials at room temperature for which the equation was first proposed (ref. 27). The cryogenic data points fall well within the scatterband of the dots. In fact, the cryogenic data fit the universal slopes equation somewhat better than do the room temperature data, as shown in the inset table in the lower part of the figure. For example, in the case of the cryogenic data,

44 percent of the life predictions were correct to within a factor of 1.5, compared to only 37 percent of the ambient temperature data.

We are encouraged by the above results, and we plan to continue our studies of cryogenic fatigue with various materials and under a variety of environmental and loading conditions.

Fracture control - The study of Fracture Mechanics has for many years been a major effort at our Laboratory. In particular, the work of Brown and Srawley (refs. 29 and 30) directed at establishing valid standard tests for determining crack propagation resistance in brittle materials, is well known. In relation to the space shuttle, we are concerned with two types of components -- thin section pressure vessels and heavy sections. In both cases, one of the important problems is to establish fracture criteria for part-through cracks since such cracks are the type more commonly found in finished hardware, and since the stress analysis procedures for such flaws are less well-developed.

Figure 30 shows some results that have recently been obtained by T. W. Orange of our Laboratory and his co-workers on 1.5 mm (0.06 in.) sheet of 2014-T6 aluminum in liquid hydrogen (refs. 31 and 32). For flat tensile specimens, as shown in Figure 30(a), the points for the surface crack lie on the same curve as those for through-the-thickness cracks, and the governing fracture stress is predominantly the crack length. For pressurized cylindrical tanks at liquid nitrogen temperature, there is an appreciable difference in strength depending on the crack depth, as seen in the results of W. S. Pierce in Figure 30(b).

Figure 31 shows some results at liquid hydrogen temperature with tensile specimens of a titanium alloy of about the same thickness as the aluminum tensile specimens of Figure 30(a). In this material, there is an appreciable difference between strengths of surface-cracked specimens with different crack depths and through-the-thickness-cracked specimens. The effect depends substantially on the depth of the crack and its length.

It is apparent, therefore, that the effect of part-through cracking depends not only on material but also on crack geometry. One of our major efforts at the present time is to establish suitable relations among geometrical, material, and stress factors for a large range of conditions that would embrace practical cases encountered in the space shuttle as well as in other applications. In this connection, we are making use of a new high-load cryogenic tensile test facility which has recently been constructed at our laboratory. A photograph of the facility is shown in Figure 32. The load capacity of the machine is 5.3 MN (1.2 million pounds). It has a cryostat suitable for testing specimens in a liquid hydrogen environment. With this facility we can test the very large specimens needed to insure plane strain conditions on which current stress intensity (K_{Ic}) analyses are based. Many safety features have been incorporated to make the tests possible with a minimum of hazard to personnel. For example, it was necessary to minimize the size and mass of the test specimen and its loading train in order to minimize cryogen requirements and increase safety.

The special specimen and loading grips shown in the insert were developed by J. L. Shannon of our Laboratory for this purpose.

The program presently being undertaken is intended to study the effects of surface crack size and shape on the fracture characteristics of several materials at liquid hydrogen temperature. An outline of the first study is shown in Figure 33. For the 2014-T651 aluminum alloy, using specimens of 15 x 2.5 cm (6 x 1 in.) cross section we shall study a range of crack sizes and shapes shown in figure 33(a). Our program will determine if it is possible to correlate the results onto one curve as shown in figure 33(b) using a shape factor Q which will depend on crack depth and length. Based on this study and similar studies on other materials we expect eventually to determine whether a shape factor Q exists that can be analytically expressed in terms of crack depth and length; if not, a more complicated procedure for design analysis may be required. Even if a functional relation for Q can be found for one material, will it be valid for others? Answers to these and other questions should make it possible to set standards for various classes of materials that can be used for acceptance tests or for design and failure analysis. These results will be extremely useful in space shuttle and other applications.

Surface thermal protection systems - We turn now to the high temperature end of the space shuttle project. Figure 34 shows the approximate temperature distribution upon re-entry of one concept of an orbiter. (Again, of course, no designs have been finalized.) Because of the high temperatures involved, and because of the presence

of oxygen, we face an oxidation problem. Several alternatives are being examined at our Laboratory, among them coated refractory metals such as columbium and tantalum, and TD-NiCr (hopefully, not requiring a coating). I shall concentrate my further remarks on our TD-NiCr program. This work is being conducted under the leadership of R. W. Hall.

The initial choice of TD-NiCr for use in the 950C (1750F) to 1204C (2200F) range was based on data such as those shown in Figure 35 which presents the specific weight change as a function of temperature for a number of alloys (ref. 33). However, this figure is based on static furnace data, wherein the chromium evaporation problem referred to previously is minimized. More realistic performance under conditions likely to be encountered in space shuttle service is shown in Figure 36 (ref. 34). Under high gas velocity and low static pressure, the rate of metal removal is tripled. In addition to surface removal, interior porosity develops, as already discussed in connection with Figure 24. Thus, as discussed previously, we are directing a major effort to improve oxidation resistance by adding aluminum to the alloy.

For the past year, we have strongly supported the Fansteel Company (now the proprietors and developers of the material originally developed by the DuPont Company) in an effort to upgrade the reproducibility and quality of the alloy. We can now routinely obtain 46 x 92 cm. (18 x 36 in.) sheets in thicknesses from 0.025 to 0.102 cm. (.010 to .040 in.), and on an experimental production basis, we have obtained sheets as large as 61 x 150 cm. (24 x 60 in.) in these thicknesses. Quality

factors, such as uniformity and sheet flatness, have been substantially improved. Uniformity and quality control have also permitted us to raise ductility at 1100°C (2000°F) from about 2% to 6% elongation. And, of course, we are now improving the oxidation resistance by incorporating aluminum into the alloy. While there is no certainty that the modified TD-NiCr, the development of which we are supporting, will emerge as the successful contender for usage as the high temperature thermal protection material (since refractory alloys and non-metallic systems are also under evaluation), the advancement of the state-of-the-art of this material is likely to pay dividends--whether for this or for numerous other potential applications.

Nuclear Space Power

Looking to the more distant future than that involved in the space shuttle, we envision a need for a nuclear space power system. Since the mission for such a system has not been definitely established, our efforts have been directed toward the concepts involved, rather than on firm specifications. Our main effort has been concentrated on a fast-spectrum reactor concept of about two megawatts thermal power (ref. 35). Such a reactor might find use in a large manned orbiting station, a manned lunar station, or possibly even for electric propulsion.

The materials requirements for such a reactor are very stringent. Being a heat source, high temperatures (>850°C or 1560°F) are desirable to obtain good thermal efficiency. Also, a higher radiator temperature

is desirable because radiators can reject heat approximately as the fourth power of temperature. Long lifetimes--of the order of 50,000 hours--are desired. Liquid metals are likely candidates as heat transfer fluids, but their metallurgical interaction with the containment materials must be minimized. The structural metals must be resistant to deformation or deterioration resulting both from loads and from radiation. Several potential compatibility problems must be solved.

The evolution of the design and selection of materials for the reactor concept now being pursued at our Laboratory followed a logical path, starting with the choice of a liquid metal. As shown in Figure 37, only lithium develops moderate pressures in the vapor state at the desired temperatures in the range above 1000°C (1830°F). Although other metals such as sodium and potassium are not completely excluded, they would involve higher pressure systems with attendant containment problems resulting from the high stresses. Selection of a nuclear fuel is, in part, based on compatibility problems with lithium. As seen in Table VI, uranium nitride best suits this purpose. In addition, it has a high melting point, high thermal conductivity

TABLE VI - CHARACTERISTICS OF NUCLEAR FUELS

	UO_2	UN	UC
Melting Point	2870°C (5200°F)	2840°C (5150°F)	2400°C 4350°F
Uranium Density, GM/CC	9.7	13.5	13.0
Thermal Conductivity, CAL/CM/DEG-SEC	0.01	0.06	0.04
Fission Gas Release	High	Low	Low
Compatibility With Lithium	Poor	Very Good	Good

(which minimizes hot spots), a high density of uranium, and a low fission gas release rate. Thus, our research has concentrated on UN as a nuclear fuel.

Next we must make the choice of a fuel containment metal. In discussing this choice, it is again possible to make reference to our technology transport principle. As we see in Table VII, the best alloys

TABLE VII - SELECTION OF CLADDING FOR FUEL PIN

Criteria	Best Alloys
Compatibility with Lithium	Cb, Ta, Mo, W
Compatibility with UN	Mo, W (use Ta with W liner)
Creep Strength	Ta, W
Fabricability and Ductility	Cb, Ta
Commercial Availability	Cb, Ta, Mo

that present themselves for possible application here are those involving the refractory metals columbium, tantalum, molybdenum, and tungsten. Although much research on these alloys was spurred by the application involved here, we already were heirs to fruits of massive investments in research on refractory metal alloys for applications that preceded this one. Among the first was the Dyna-soar program, an aeronautical vehicle, which was to fly partly in space and partly in the atmosphere. High reentry temperatures spurred extensive national programs in refractory alloy

development. Later, as we became interested in liquid metal reactor systems, we learned of the excellent compatibility between liquid metals and certain refractory metal alloys, which is a required property together with good high temperature creep strength. Therefore, for the 1000°C (1830°F) range involved in the reactor that I am discussing, we naturally looked to the refractory metals. The state of development of these alloys is far more advanced as a result of spurs arising out of earlier potential applications, some of which never reached fruition. Nevertheless, the value of that materials research was conserved.

Returning now to Table VII, we see that the tantalum alloys offer the best promise when all factors involving compatibility with lithium, creep strength, fabricability and ductility, and commercial availability are considered. Their only disadvantage is incompatibility with the uranium nitride fuel. Tungsten, which is compatible with uranium nitride, can be used as a liner to prevent contact of the fuel with the tantalum containment. Our choice of a tantalum alloy was T-111 which has the basic composition Ta-8W-2Hf. Although originally developed under Navy sponsorship, we have provided considerable funding for both the development of this alloy and the determination of its properties.

A schematic diagram of the fuel element as it has been developed at our Laboratory (under the leadership of N. T. Saunders, R. E. Gluyas, and their coworkers) is shown in Figure 38. It consists of UN as the fuel, T-111 as the container (cladding) material, and a tungsten liner to separate the UN from the T-111. Summaries of our technology program

and current results are given in Tables VIII and IX, respectively. I shall not discuss these tables at length; for a detailed description, reference may be made to a recent report (ref. 36).

Some of the research with the fuel elements is done within our own Laboratory, some at a near-by NASA materials test reactor (at Plum Brook near Sandusky, Ohio), and some under contract. For example, General Electric has been conducting a pumped-loop investigation for us, as shown in Figure 39. In addition to the fuel element components as discussed above, the pumped-loop contains some TZM (a molybdenum alloy containing titanium and zirconium) because the alloy is used for certain structural parts of the reactor (e.g., the reflector). The inset in Figure 39 shows the appearance of the fuel elements after 7500 hours of testing. It shows no evidence of corrosion, and we are very heartened by the results obtained to date.

TABLE VIII - MATERIALS TECHNOLOGY PROGRAM
FOR NUCLEAR FUEL ELEMENT DEVELOPMENT

Fabrication Process Development
1. UN Fuel Forms
2. W-Liner in T-111 Tubing
3. T-111 Components and Assembly of Fuel Pins
Out-Of-Pile Capsule and Pumped-Loop Studies
1. UN/T-111 Compatibility
2. Effectiveness of W-Liner
3. UN/Lithium Compatibility
4. Corrosion of T-111 by Lithium
Irradiation Tests
1. Fuel Pins
Compatibility of Materials
Fission Gas Release
Swelling
2. Refractory Metals
Swelling
Effect on Ductility

TABLE IX - CURRENT RESULTS OF FUEL ELEMENT PROGRAM

Fabrication of Fuel Pins

1. UN fuel forms (of <300 ppm oxygen and free of defects) can be routinely prepared.
2. T-111 tubing is lined with tungsten by a differential thermal expansion method.
3. Machining of T-111 components and fuel pin assembly and welding present no serious problems.

Out-Of-Pile Compatibility Studies

1. UN and T-111, not compatible in direct contact at 1040°C (1900°F). No reaction if separated by 0.013cm (0.005 in.) thick tungsten.
2. UN with <300ppm oxygen is compatible with lithium at 1040°C (1900°F).
3. No contamination or corrosion of simulated fuel specimens after 75 hours at 1040°C (1900°F) in a pumped-lithium loop.

Irradiation Tests

1. Most tests are underway but not complete.
2. So far, fission gas release appears to be low: less than 1% after 1 A/O burnup in 1500 hours at about 1000°C (1830°F).
3. No irradiation-induced compatibility problems apparent.
4. Greatest unknown is effect of fast neutron irradiation on T-111.

LIFE PREDICTION PROBLEMS

High temperature life prediction problems arise in all of the applications I have previously discussed, so it is appropriate that the subject be treated as a separate entity, rather than in the context of any one of them. Because of the special personal interest I have maintained in this area of research, I am tempted to discuss the subject at length;

however, because of the time limitations I am forced to keep my remarks brief, and limited to new results derived in the very recent past. Thus I will comment only on three new developments: a) a new time-temperature parameter being studied for correlation and extrapolation of creep-rupture data, b) high gas-velocity effects on creep-rupture, and c) a new approach we are studying for treating creep-fatigue interaction.

Time-Temperature Parameters

Time-temperature parameters are commonly used for the correlation and extrapolation of creep and creep rupture data. Many parameters are used, among the most common being those of Larson-Miller (ref. 37) in the form $(T + 460)\ (C + \log t)$, Manson-Haferd (ref. 38) in the form $\frac{\log t - \log t_a}{T - T_a}$, and Orr-Sherby-Dorn (ref. 39) in the form $\log t + \frac{C}{T + 460}$. Other parameters are summarized and discussed in references 40 and 41. While many investigations have been conducted to determine the relative merits of the various parameters, the question is still not completely resolved. Some investigators have maintained that no parameter is suitable for the extrapolation of some materials, notably those that exhibit structural instabilities. Glen (ref. 42) has cited silicon-killed carbon steel as an example of such a material, and Goldhoff and Hahn (ref. 43) have cited the nickel-base alloy Astroloy as another example.

In order to circumvent the problem of which form to use in representing the time-temperature relation we have recently (refs. 40 and 44) suggested a parameter in very general form

$$\log t + AP \log t + P$$

where A is a material constant, and P is a function of temperature. It is shown in ref. 44 that by simple algebraic manipulation any one of the commonly used time-temperature parameters can be expressed as a special case of this parameter by the proper choice of A and P. Thus it is not necessary to commit ourselves in advance as to which of the commonly used parameters is the most suitable; use of the new parameter essentially embraces them all, and the best one will emerge when the proper values of A and P are established. Even more important is that by special choices of A and P the new parameter lends itself to forms not equivalent to any of the common parameters. Therefore, material behavior not predictable by the common parameters might still be explainable on the basis of the new parameter.

The problem, of course, is to determine the values of the constant A and the temperature function P. In references 40 and 44 this question is discussed, using in the analysis least-squares procedures and "station-function" concepts which reduce the need for pre-judging the analytical form of the functions involved. We are still working on this problem, seeking simple and objective procedures. At this time I cannot present any final conclusions. It does appear, however, that it is not always possible to find the best constants and functions by considerations of least-squares procedures using only data in the short time range. It may be necessary to include in the analysis some metallurgical information relating to the long-time stability of the material. Perhaps this can be achieved by relating the constant A to material stability, and extablishing the function P on the basis of only least-squares techniques.

The important fact we have learned recently after studying a great many materials for which long-time data are available is that in all cases there exists a constant A and temperature function P for which short-time data could be extrapolated to long time behavior. Fig. 40 shows the results for Glen's carbon steel and Goldhoff and Hahn's Astroloy. In each case the value of A is -0.16. Short time data were used, as shown in the figure, to extrapolate long time behavior. The results are good based on the new parameter, whereas conventional parameters were not satisfactory, according to Glen, and Goldhoff and Hahn. Perhaps the new parameter will be useful in the treatment of unstable as well as stable materials. It remains as yet to establish the best procedures for determining the proper values of A and P for each material using only information that can be obtained in a relatively short time. Simplifications are also being sought. Hopefully we shall be able to report results in the near future. In connection with this work I wish, especially, to acknowledge the diligent and able assistance of C. R. Ensign.

Gas Impingement Effects on Creep Rupture Life

Most creep rupture data are generated in a static heated air environment. Yet application of some of these data involve high velocity gas flows. It is known that the surface influences strength characteristics substantially, especially if there is an oxidation-corrosion interaction with the flowing air.

D. A. Spera and his co-workers at our laboratory have in recent years been developing a method for predicting the thermal fatigue endurance of gas turbine blades (refs. 45 to 49). With this method, cyclic life is calculated from static tensile and creep-rupture data. They recognized the possibility that high-velocity gas impingement could substantially reduce creep rupture strength, and so have recently undertaken an extensive study of this phenomenon. Figure 41 shows their apparatus. A burner is provided to burn jet engine fuel in air, and the combustion gas is ejected through a nozzle at velocities up to Mach 1, corresponding to velocities encountered in gas turbines.

Some of their results to date are shown in Figure 42. Here, as a function of temperature, are plotted the ratios of creep-rupture life in a Mach 1 stream to creep-rupture life in a static furnace at the same stress and temperature. It can be seen that at temperatures above 871°C (1600°F), the loss of creep rupture life can be very substantial. At about 982°C (1800°F), the life is reduced by a factor of 10, and at about 1066°C (1950°F), it is reduced by a factor of 20. The data are for two nickel base alloys: B-1900 with an aluminide coating, and IN-100 without a coating. For the coated material the reduction is even greater than for the uncoated material. The drastic reduction in creep rupture life observed here commands a re-evaluation of the direct applicability of furnace test data to high temperature, high velocity service application. Similar results have recently been obtained in Russia using cold air impingement on specimens heated by electrical self-resistance (refs. 50 and 51.)

Creep - Fatigue Interaction

I shall conclude my lecture with a few remarks on recent research we have conducted on creep-fatigue interaction at high temperature. It is particularly appropriate that I comment on this subject at this time. First, of course, is the fact that it is a very significant subject, closely pertaining to the theme of this conference and to the one on Thermal Fatigue which follows it. Second, is that we have recently undertaken a new approach, and I am pleased to be able to report some results. And, third, is a somewhat personal matter. It was about 8 years ago when I chaired a session at a conference on High Temperature Structures and Materials at Columbia University that I had the pleasure of first meeting and introducing Professor Shuji Taira who, in his paper (ref. 52), discussed the idea of treating creep-fatigue interaction by using a generalized linear damage rule — cycle ratios to represent fatigue damage, and time ratios to represent creep damage. Much good use has been made of his idea in the last decade. Six years ago I visited Japan to present a general lecture at the First International Conference on Fracture, at which time I first presented (ref. 53) the concept that accounts for creep-fatigue interaction considering intercrystalline cracking as a process of bypassing a large part of the crack initiation phase and part of the crack propagation phase. I termed the approach the "10-percent rule", and it, too, has found considerable application in the intervening years. I should now like to discuss briefly our new approach which is intended to overcome some of the limitations of other methods of analysis that have become apparent as a result of further study.

The "strain-partitioning approach" as we call it (ref. 54), is based on the distinction between two forms of inelastic strain—plastic strain and creep strain. Plastic strain is governed principally by slip and is concentrated in the slip planes; creep is principally diffusion-controlled and a large component of it may be concentrated in the grain boundaries. An important feature of the method is to draw a further distinction between the manner in which tensile inelastic strain is reversed by the compressive inelastic strain to establish a closed hysteresis loop. In some cases tensile plastic flow is reversed by compressive plastic flow, or tensile creep is reversed by compressive creep. In other cases, however, tensile creep may be reversed by compressive plastic flow, or tensile plastic flow may be reversed by compressive creep.

Thus, there are four basic strain reversal possibilities, each of which is designated according to a subscript system in which the first letter designates the type of tensile strain, and the second the type of compressive strain (c for creep, and p for plastic flow). These four are:

$\Delta\varepsilon_{pp}$ - tensile plastic flow reversed by compressive plastic flow
$\Delta\varepsilon_{cc}$ - tensile creep reversed by compressive creep
$\Delta\varepsilon_{pc}$ - tensile plastic flow reversed by compressive creep
$\Delta\varepsilon_{cp}$ - tensile creep reversed by compressive plastic flow

In this brief outline it is not possible to describe in detail the type of tests required to establish how each of the above affects cyclic life; a complete description may be found in the recent paper co-authored by myself, G. R. Halford, and M. H. Hirschberg (ref. 54). It is sufficient to point out that, for a given applied inelastic strain the cyclic life can vary appreciably depending on which of the above four types of strain predominates. Figure 43 shows the partitioned strain range-life

relations for Type 316 stainless steel at 705°C (1300°F). It is seen that for this material the most damaging type of strain is $\Delta\varepsilon_{cp}$, wherein creep in tension is reversed by compressive plastic flow. The life for a given amount of strain range of this type is less than 1/10 of the life achieved when the same strain range is applied as $\Delta\varepsilon_{pc}$, wherein the creep is in compression and plastic flow is in tension.

Figure 44 shows the physical basis behind the drastic differences in life associated with the two types of strain $\Delta\varepsilon_{cp}$ and $\Delta\varepsilon_{pc}$. The strain ranges for the two tests were about the same ($\Delta\varepsilon_{cp}$ was even smaller at 1.47%, compared to the 1.62% for $\Delta\varepsilon_{pc}$), yet the life for $\Delta\varepsilon_{cp}$ was only 15 cycles, while the life for $\Delta\varepsilon_{pc}$ was 264 cycles. When the tensile component was creep ($\Delta\varepsilon_{cp}$), the failure surface was predominantly intercrystalline, and the whole region in the vicinity of the fracture section showed intercrystalline cracking. When the tensile component was plastic flow ($\Delta\varepsilon_{pc}$), no intercrystalline cracking was apparent, and the failure area resembled that of specimens tested in conventional high-strain, low-cycle fatigue.

Having recognized that life is affected by the type of strain and manner of reversal, the "strain-partitioning" method seeks to partition an imposed strain range into the four possible components described above. Each strain component is associated with a given life, according to curves such as shown in figure 43. Thus, in one cycle of loading, the damage produced by each strain component can be taken as the reciprocal of the life determined from the curve. The total damage per cycle is

taken as the linear sum of the damage due to each component strain range, and the net life is determined from a linear damage rule. Figure 45 summarizes how well the procedure works for Type 316 stainless steel. Plotted are experimental lives for each of a variety of laboratory tests, versus the life predicted from the relations of figure 43. The agreement is extremely good, being within a factor of two on life.

The strain-partitioning method outlined above has only recently been introduced by us, and although we are enthusiastic about its possibilities, we feel that we must study the method further to determine its strengths and weaknesses. It is a "new direction", but how far it will take us must yet be established. Many opportunities appear on the horizon, however. For example, it may be possible to estimate the lines such as shown in figure 43 from simple creep-rupture and tensile tests in somewhat the same manner as we estimate the elastic and plastic lines in room-temperature fatigue when applying our "universal-slopes method" (ref. 27). We recognize that even after these lines are established, their use may be complicated, in practical cases, by the difficulty of determining the total inelastic strain and the four partitioned components. The analysis required for an accurate partitioning may indeed involve complex computations. But the method has the advantage of suggesting bounds on life, using as extremes the most optimistic and most pessimistic of the lines in the life relations shown in figure 43. In fact, in reference 54 we have attempted to provide an explanation of why our "10-percent rule" has worked so well in so many cases, using as

a basis the "bound" concept referred to above. Thus, even if no accurate analysis is possible, a good estimate may be made by the method.

A third advantage that the method may offer is that it may reduce the amount of data and analysis required when the application involves non-uniform temperatures. It is quite possible that the life relations, such as shown in figure 43, are relatively insensitive to temperature. The apparent temperature-sensitivity of fatigue may, in fact, be due to different partitioning of an imposed strain, dependent on the temperature and other test parameters. Thus, a given strain imposed at a low temperature may be absorbed mainly as $\Delta\varepsilon_{pp}$, whereas at a higher temperature more of it will become $\Delta\varepsilon_{cc}$. However, the life relations for the individual components $\Delta\varepsilon_{pp}$ and $\Delta\varepsilon_{cc}$ as well as for $\Delta\varepsilon_{cp}$ and $\Delta\varepsilon_{pc}$ may not be very sensitive to temperature. That this may, indeed, be the case is reflected in figure 46. Here the life relationships for two materials — Type 316 stainless steel and 2 1/4Cr-1Mo steel — were determined from life data at one temperature, and demonstrated to be valid at other temperatures as well. For the Type 316 stainless steel, the lines for 705°C (1300°F) shown in figure 43 were used. Cyclic lives were then predicted for various types of tests run at 595°C (1100°F), 650°C (1200°F) and 815°C (1500°F). The life relationships for the 2 1/4Cr-1Mo steel were determined at 595°C (1100°F) and cyclic lives were predicted for tests conducted at 510°C (950°F), 565°C (1050°F), and 650°C (1200°F). As seen in the plot, the predictions were accurate to within a factor of 2 in nearly all cases. Imagine how much additional data would have been required

to predict the fatigue lives if the basis of computation were life fractions based on time at stress rather than on partitioned strain range! The implications regarding possible simplifications in thermal fatigue analysis, wherein continuous changes in stress and temperature occur, are self-evident.

CONCLUDING REMARKS

Gentlemen, I have tried to outline some new directions which we are pursuing at our Laboratory to solve important materials problems limited by stringent requirements. I have not tried to be all-inclusive because of time limitations. Even the sampling used shows, however, that materials impose severe restrictions on how we can solve many technological problems that face us. I have emphasized the need for Conferences such as this one as a means of communication of new ideas, new data, and new interpretations that can help solve these problems. I have also tried to emphasize that good research, followed by good reporting, will prove valuable - whether in the application intended when the research was done, or in some other connection; the value of the research will be conserved. I know you are all anxious to report your own new findings and to hear from others who wish to communicate theirs. Good luck to you in achieving these goals!

ACKNOWLEDGMENT

I wish gratefully to acknowledge the support of the NASA-Lewis Research Center in arranging for my participation in this Conference, to my staff of the Materials and Structures Division whose research provided the major content of this lecture, and to various staff members, especially John C. Freche who provided invaluable assistance in the preparation of the report.

REFERENCES

(1) Gordon, W. A. and Chapman, G. B., Spectrochem. Acta, 25B, 123 (1970).

(2) Oldrieve, R. E. and Saunders, N. T., Aerospace Structural Materials, NASA SP-227, 317 (1970).

(3) Oldrieve, R. E. and Blankenship, C. P., Proposed NASA TN.

(4) Jones, J. I., Macromolec. Sci., C2, 303 (1968).

(5) Hanson, M. P. and Serafini, T. T., Proposed NASA TN.

(6) Serafini, T. T., Delvigs, P. and Lightsey, G. R., NASA TM X-67803, (1971).

(7) Waters, W. J. and Freche, J. C., J. Eng. Power, 90, 1-10 (1968).

(8) Freche, J. C., Waters, W. J., and Ashbrook, R. L., NASA TN D-5248, (1969).

(9) Freche, J. C., Ashbrook, R. L. and Waters, W. J., Proposed NASA TN.

(10) Waters, W. J. and Freche, J. C., NASA TN D-5352, (1969).

(11) Schafer, R. J., Quatinetz, M. and Weeton, J. W., NASA TN D-1167, (1960).

(12) Norris, L. F., Reinhardt, G. and Cremens, W. S., NASA TN D-3834, (1967).

(13) Weeton, J. W. and Quatinetz, M., NASA TM X-52228, (1966). Also Oxide Dispersion Strengthening, Gordon and Breach, Science Publishers, Inc., New York, 751 (1968).

(14) Quatinetz, M. and Weeton, J. W., NASA TN D-5421, (1969).

(15) Jech, R. W., McDanels, D. L. and Weeton, J. W., Proceedings of the Sixth Sagamore Ordnance Materials and Research Conference, Rep. MET 661-601, Syracuse Univ. Res. Inst., 116 (1959).

(16) Petrasek, D. W. and Weeton, J. W., NASA TN D-1568, (1963).

(17) Petrasek, D. W., NASA TN D-3073, (1965).

(18) Petrasek, D. W., Signorelli, R. A. and Weeton, J. W., NASA TN D-4787, (1968).

(19) Petrasek, D. W. and Signorelli, R. A., NASA TN D-5575, (1970).

(20) Probst, H. B., Aerospace Structural Materials, NASA SP-227, 279 (1970).

(21) Deadmore, D. L., NASA TM X-2195, (1971).

(22) Lowell, C. E. and Drell, I. L., NASA TM X-2002, (1970).

(23) Lowell, C. E., Aerospace Structural Materials, NASA SP-227, 295 (1970).

(24) Lowell, C. E. and Sanders, W. A., NASA TN to be published.

(25) Centalanzi, F. J., NASA TM X-62015, (1971).

(26) Gedwill, M. A. and Grisaffe, S. J., NASA TM X-52916, (1970).

(27) Manson, S. S., Experimental Mech., 5, 193 (1965).

(28) Nachtigall, A. J., Proposed NASA TN.

(29) Srawley, J. E. and Brown, W. F., Jr., Fracture Toughness Testing and its Applications, Spec. Tech. Publ. No. 381, ASTM, 133 (1965). (Also available as NASA TN D-2599 (1965))

(30) Brown, W. F., Jr. and Srawley, J. E., Plane Strain Crack Toughness Testing of High Strength Metallic Materials, Spec. Tech. Publ. No. 410, ASTM, (1967).

(31) Orange, T. W., Sullivan, T. L. and Calfo, F. D., NASA TN D-6305, (1971).

(32) Pierce, W. S., NASA TN D-6099, (1970).

(33) Cole, F. W., Padden, J. B. and Spencer, A. R., NASA CR-1184, (1968).

(34) Saunders, N. T., Space Transportation System Technology Symposium, NASA TM X-52876, vol. III, 159 (1970).

(35) Krasner, M. H., Davison, H. W. and Diaguila, A. J., NASA TM X-67859, (1971).

(36) Gluyas, R. E. and Lietzke, A. F., NASA TM X-67869, (1971).

(37) Larson, F. R. and Miller, J., Trans. ASME, 74, 765 (1952).

(38) Manson, S. S. and Haferd, A. M., NACA TN 2890, (1953).

(39) Orr, R. L., Sherby, O. D. and Dorn, J. E., Trans. ASM, 46, 113 (1954).

(40) Manson, S. S., Time-Temperature Parameters for Creep-Rupture Analysis, ASM Publication No. D8-100, 1 (1968).

(41) Grounes, M., J. Basic Eng., 91, 59 (1969).

(42) Glen, J. and Johnson, R. F., Some Aspects Concerning the Extrapolation of Rupture Data, BISRA-The Inter-Group Laboratories of the British Steel Corp., London, England.

(43) Goldhoff, R. M. and Hahn, G. J., Time-Temperature Parameters for Creep-Rupture Analysis, ASM Publication No. D8-100, 199 (1968).

(44) Manson, S. S. and Ensign, C. R., NASA TM X-52999, (1971).

(45) Spera, D. A., PhD. Thesis, Univ. of Wisconsin, (1968).

(46) Spera, D. A., NASA TN D-5317, (1969).

(47) Spera, D. A., NASA TN D-5489, (1969).

(48) Spera, D. A., Howes, M. A. H. and Bizon, P. T., NASA TM X-52975, (1971).

(49) Spera, D. A., Calfo, F. D. and Bizon, P. T., NASA TM X-67820, (1971).

(50) Sorokin, V. G., Bogachev, I. N., Veksler, Yu. G., Lesnikov, V. P. and Filippov, M. A., Metalloved. Term. Obrab. Metal., No. 3, 2 (1970).

(51) Bogachev, I. N., Veksler, Yu. G., and Sorokin, V. G., Izv. Vyssh. Ucheb. Zaved. Chern. Met., No. 4, 142 (1970).

(52) Taira, S., High Temperature Structures and Materials, Pergamon Press, New York, 187 (1964).

(53) Manson, S. S., Int. J. Fracture Mech., 2, 327 (1966).

(54) Manson, S. S., Halford, G. R. and Hirschberg, M. H., NASA TM X-67838, (1971).

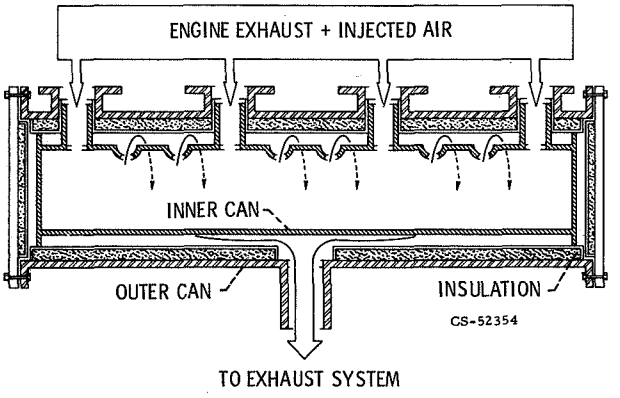

Figure 1. - Schematic of experimental automotive thermal reactor.

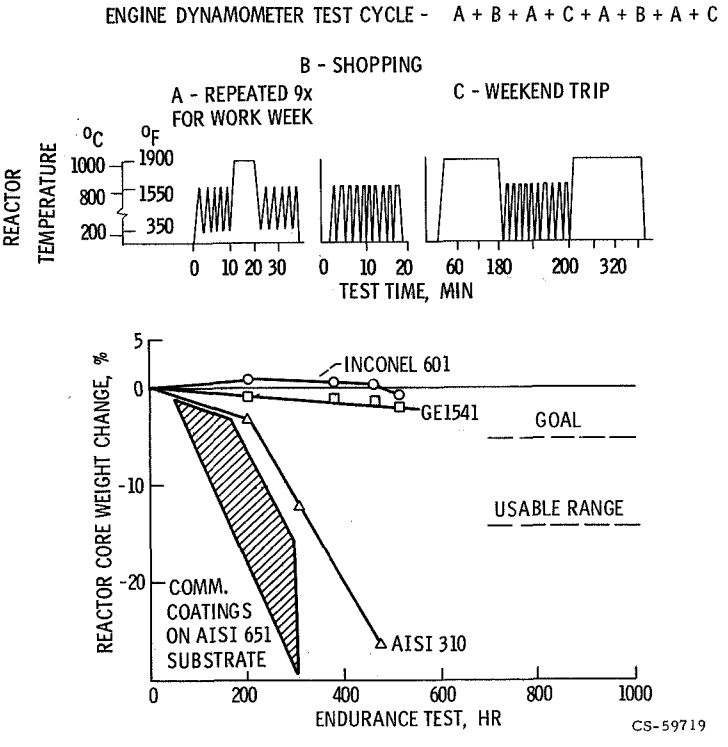

Figure 2. - Performance of alloys and coatings in automotive thermal reactor endurance tests (engine-dynamometer test).

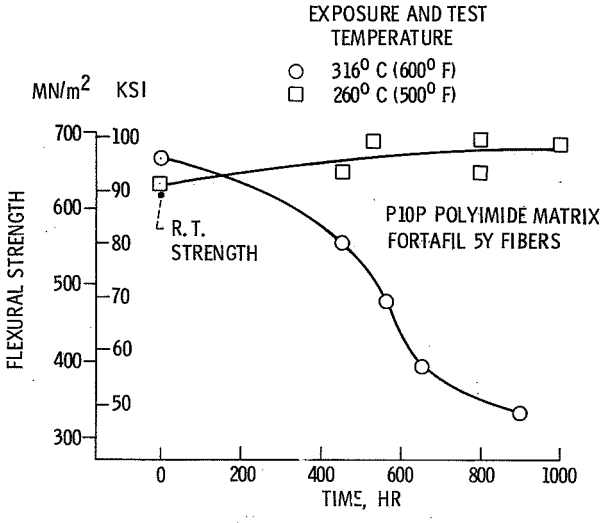

Figure 3. - Flexural strength of polymer-graphite composite exposed and tested in air at elevated temperature.

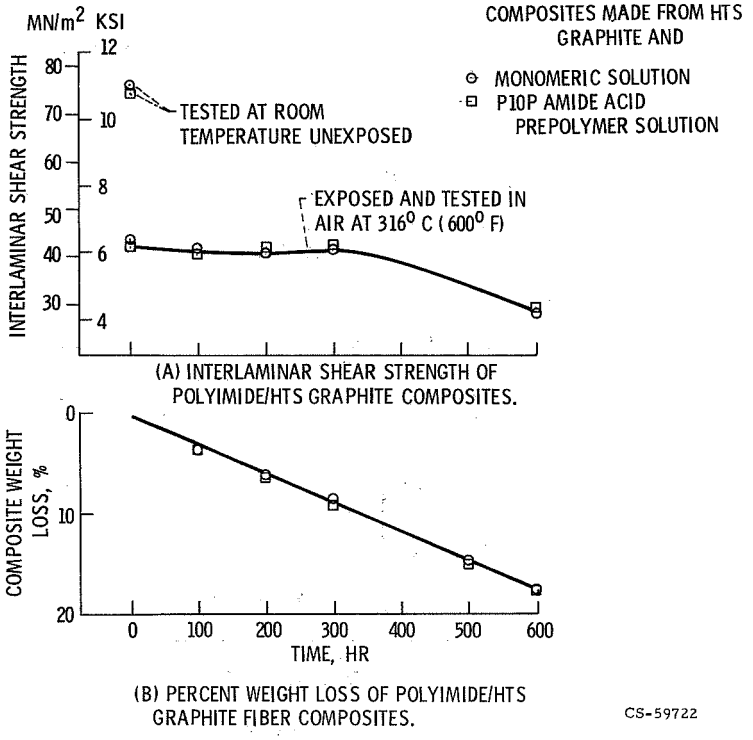

Figure 4. - Effect of temperature on properties of polyimide-graphite fiber composite.

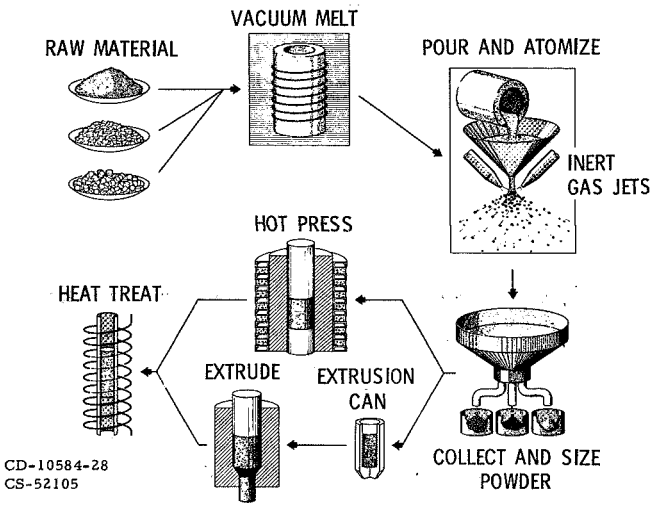

Figure 5. - Prealloyed powder processing.

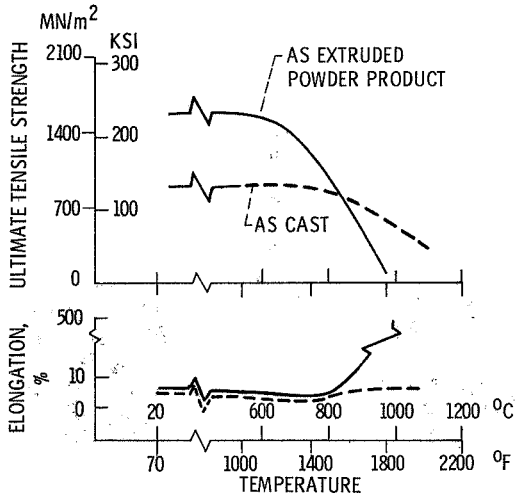

Figure 6. - Improvements in tensile properties of TAZ-8A by prealloyed powder processing.

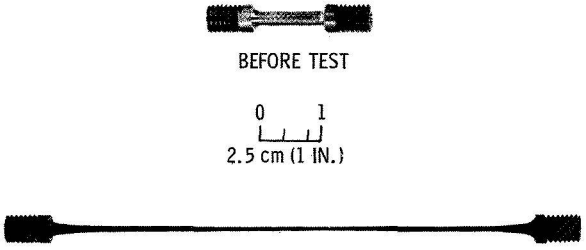

C-69-1007
CS-50263

Figure 7. - Superplasticity in as-extruded TAZ-8A powder product.

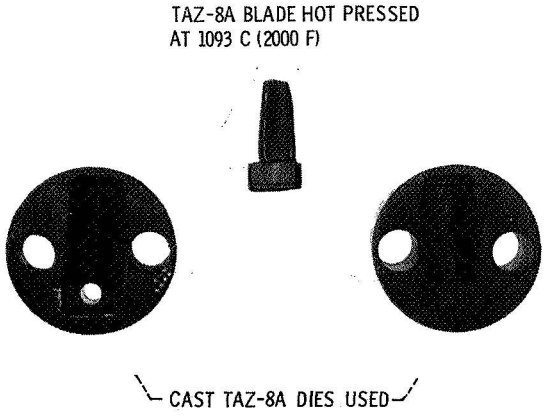

C-69-3280
CS-52106

Figure 8. - Formability of TAZ-8A prealloyed powder product.

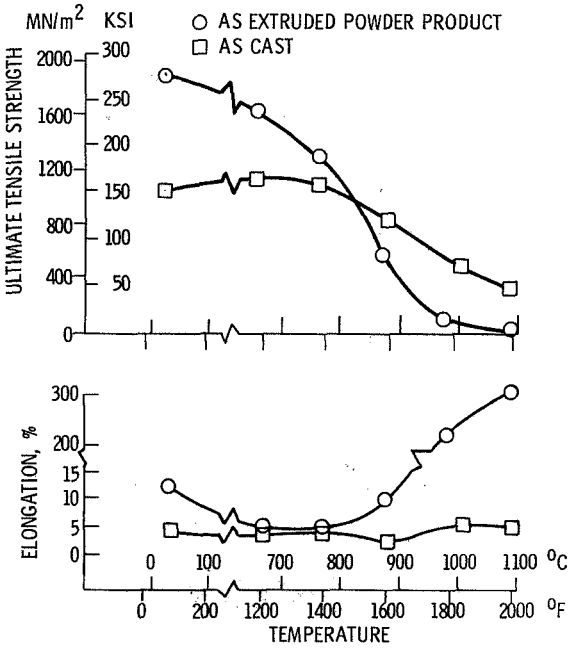

Figure 9. - Comparison of VI-A alloy tensile properties in cast and powder product form.

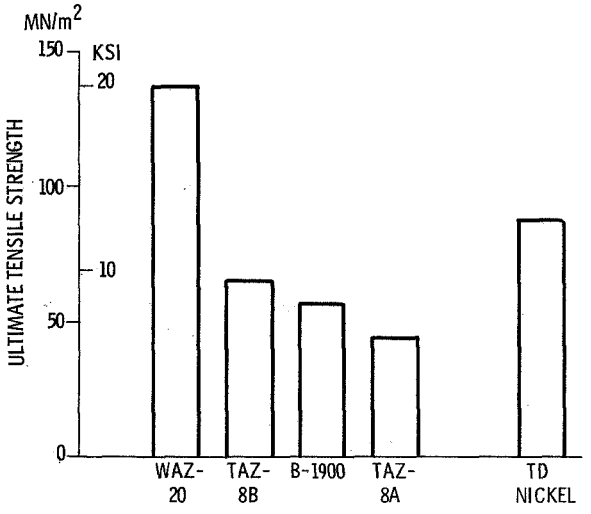

Figure 10. - Strength of nickel base alloys at 1200° C (2200° F).

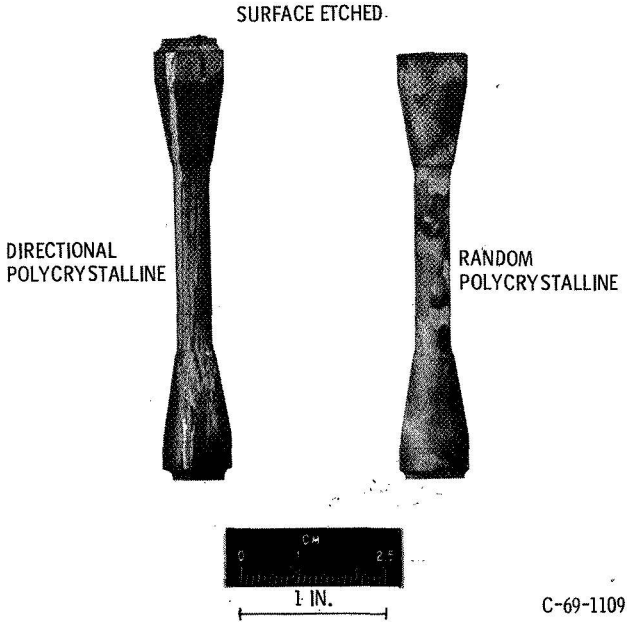

Figure 11. - Two cast forms of WAZ-20.

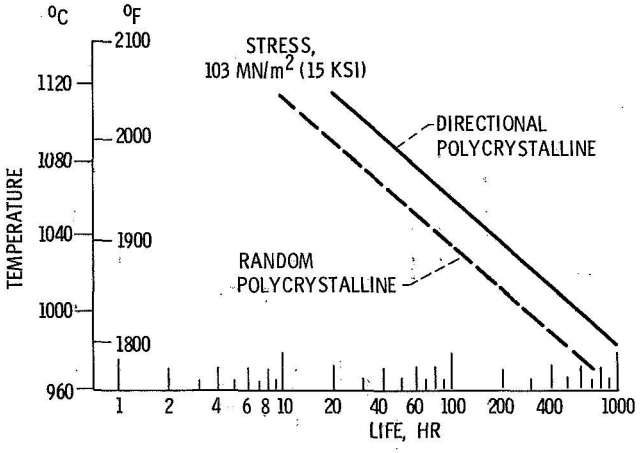

Figure 12. - Effect of directional solidification on rupture properties of WAZ-20.

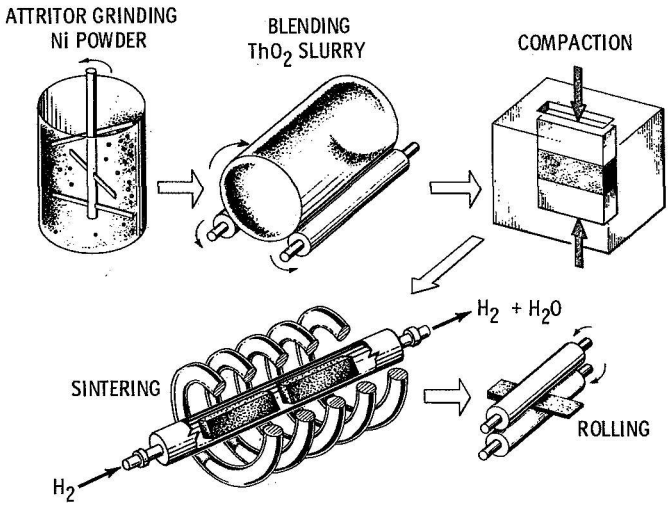

Figure 13. - NASA Comminution and Blend process for dispersion strengthening.

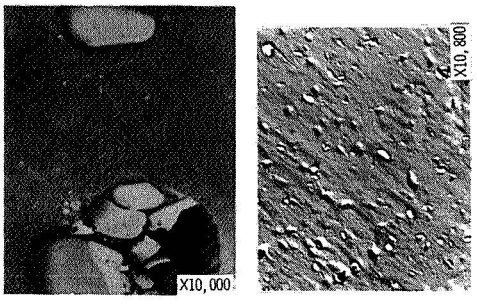

CS-40015 CS-40018

(A) AGGLOMERATED OXIDES IN UNCLEANED COMPACTS.

(B) OXIDE DISTRIBUTION USING NASCAB METHOD.

Figure 14. - Comparison of structures of dispersion strengthened Ni - Al_2O_3 materials made using NASCAB methods with those of materials made by sintering an uncleaned compact.

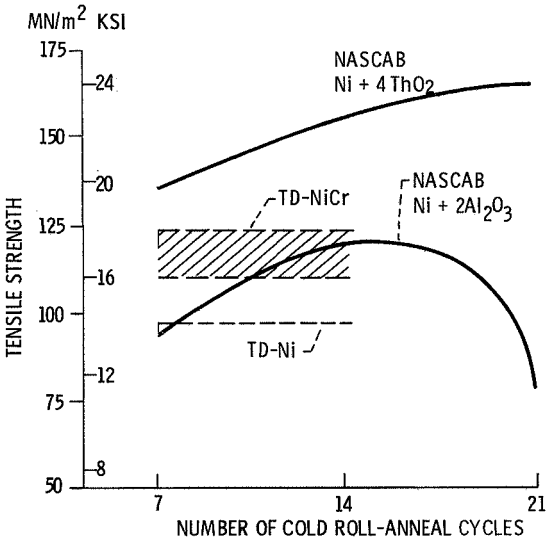

Figure 15. - Comparison of tensile strength of NASA dispersion strengthened Ni sheet with other dispersion strengthened products at 1093° C (2000° F).

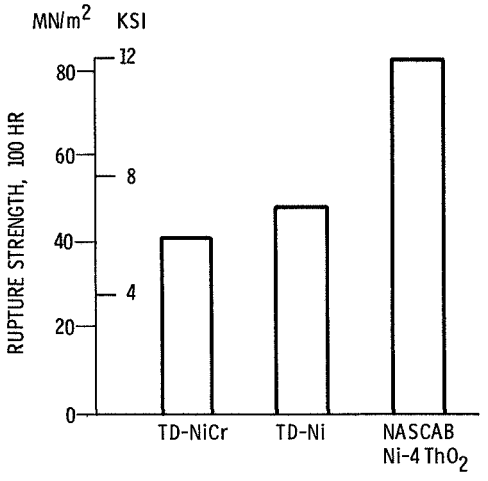

Figure 16. - Comparison of 100 hour creep rupture strength of dispersion strengthened Ni and Ni alloy sheet at 1093° C (2000° F).

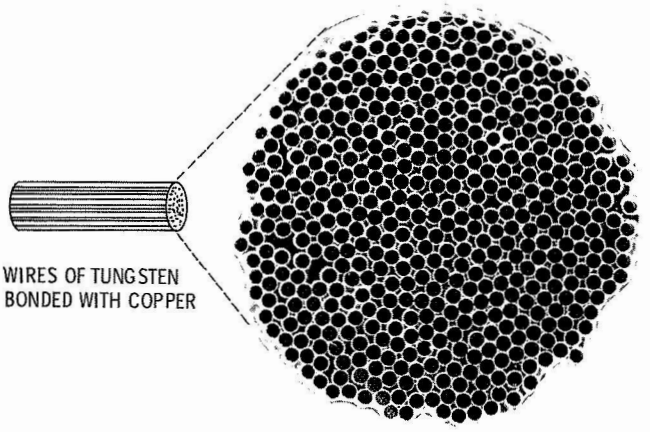

Figure 17. - Cross sectional macrostructure of tungsten fiber reinforced copper composite.

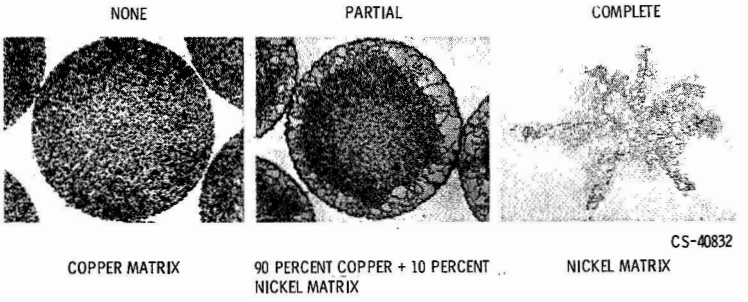

Figure 18. - Reaction in composite materials.

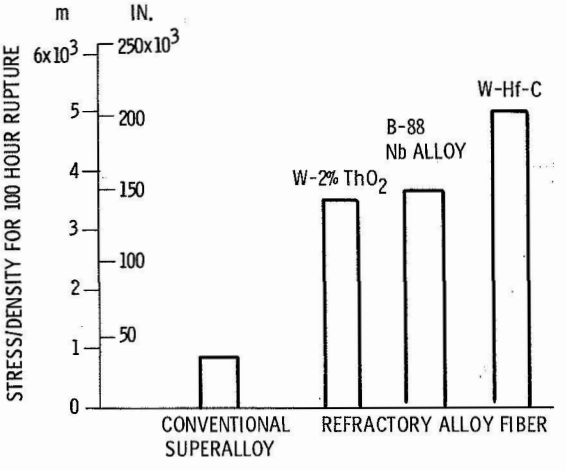

Figure 19. - Specific 100 hour rupture strength of refractory alloy fibers compared with a conventional superalloy at 1093^{0} C (2000^{0} F).

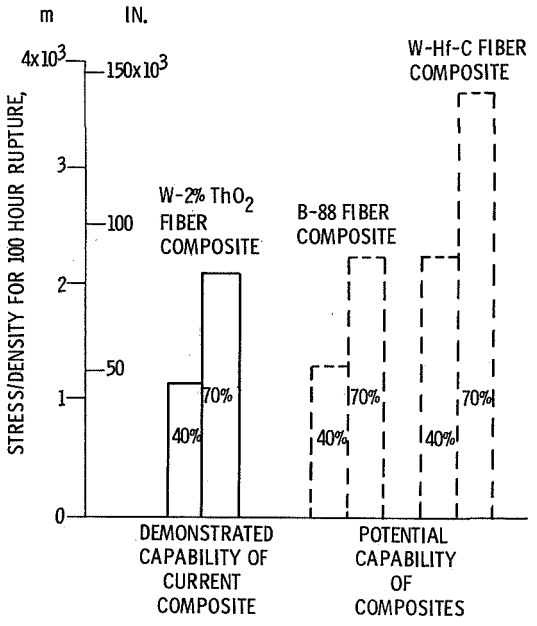

Figure 20. - Demonstrated and potential values of specific creep-rupture strengths of refractory metal fiber reinforced superalloy composites at 1093° C (2000° F).

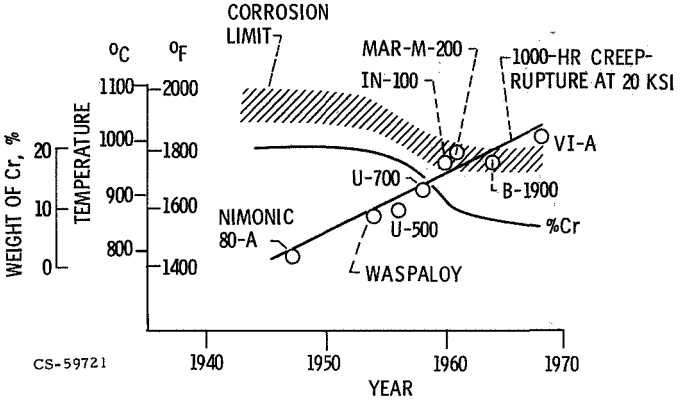

Figure 21. - Basis of corrosion barrier for nickel-base alloys.

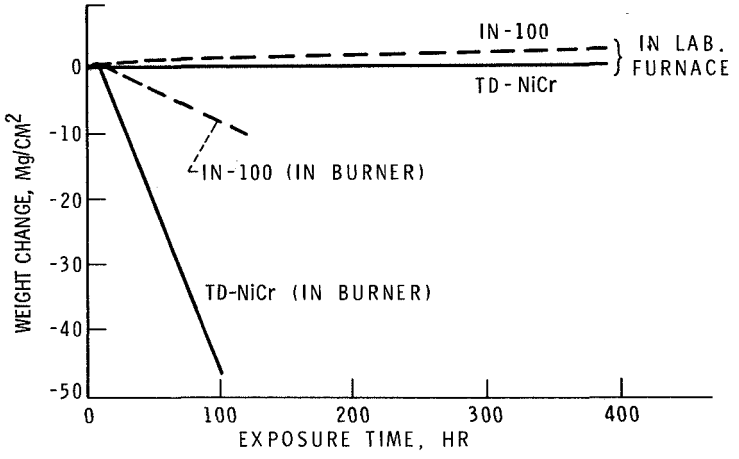

Figure 22. - Effect of gas velocity on oxidation behavior at 2000° F.

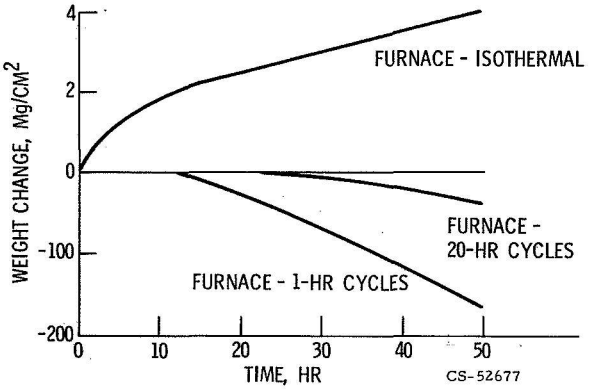

Figure 23. - Effect of thermal cycling on oxidation of alloy WI-52 at 1093 C (2000 F).

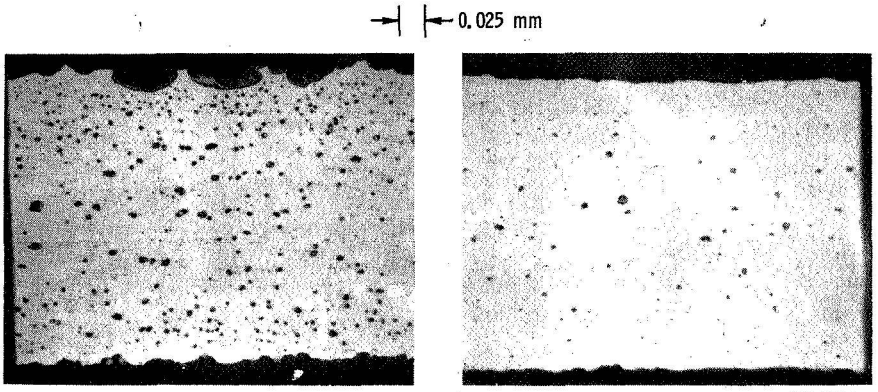

(A) TD-NiCr 50 CYCLES. (B) TD-NiCrAlY 40 CYCLES.

Figure 24. - Microstructures of TD-NiCr and TD-NiCrAlY after arc-jet exposure at 1204° C (2200 F), 15 torr. 1 cycle = 30 minutes at temperature.

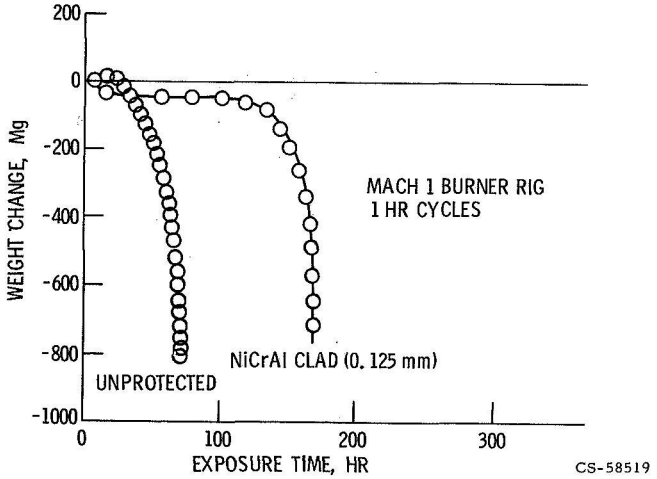

Figure 25. - Effect of 0.125 mm cladding on oxidation resistance of TD-NiCr at 1056 C (1925° F).

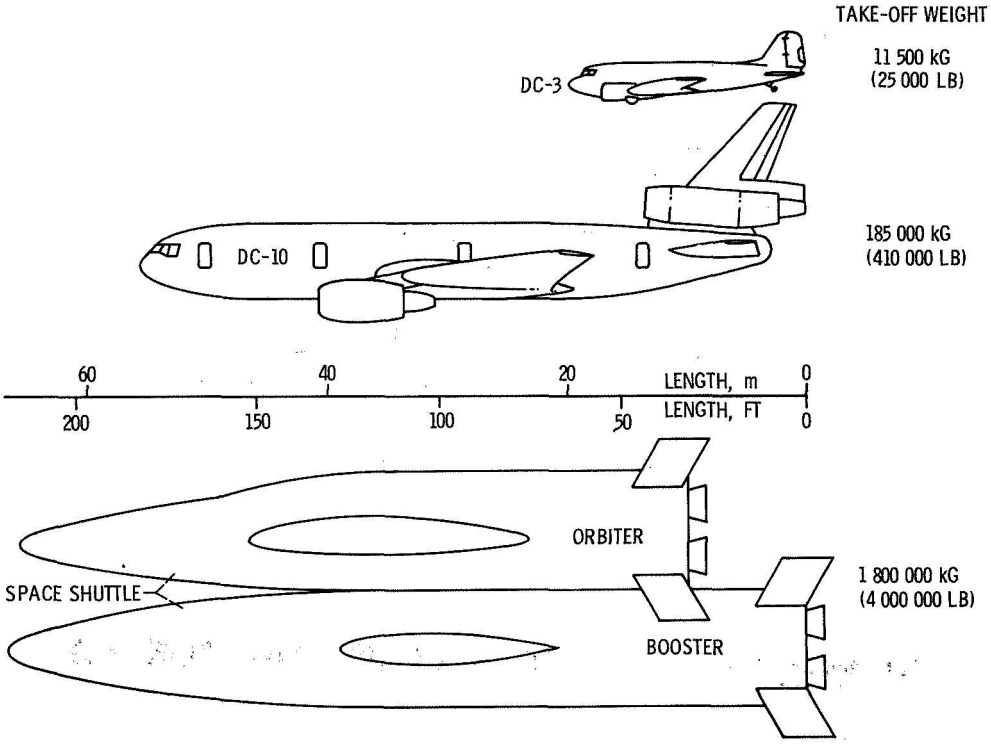

Figure 26. - Comparison of space shuttle size with commercial aircraft.

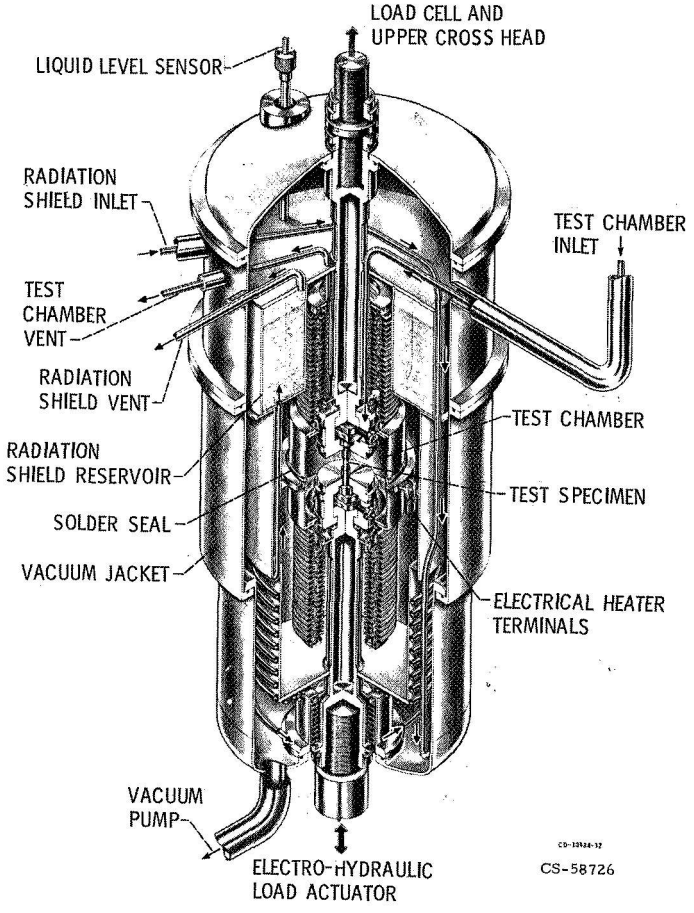

Figure 27. - Cryostat used for tensile testing and fatigue testing.

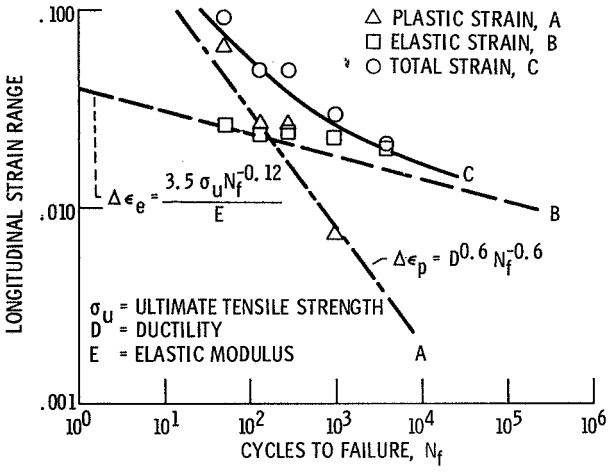

Figure 28. - Comparison of predicted and experimental fatigue behavior for strain-cycled titanium-5 Al-2.5 Sn specimens in liquid helium.

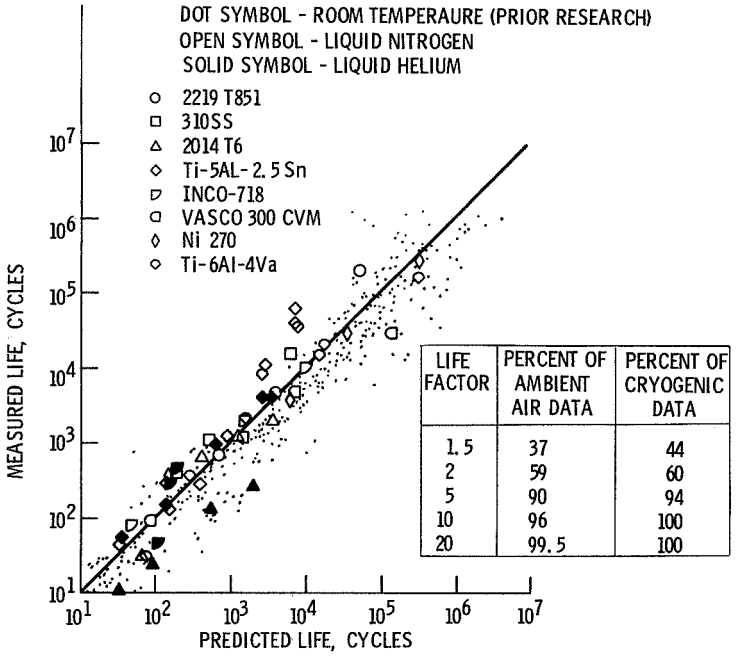

LIFE FACTOR	PERCENT OF AMBIENT AIR DATA	PERCENT OF CRYOGENIC DATA
1.5	37	44
2	59	60
5	90	94
10	96	100
20	99.5	100

Figure 29. - Application of the equation of universal slopes to cryogenic fatigue.

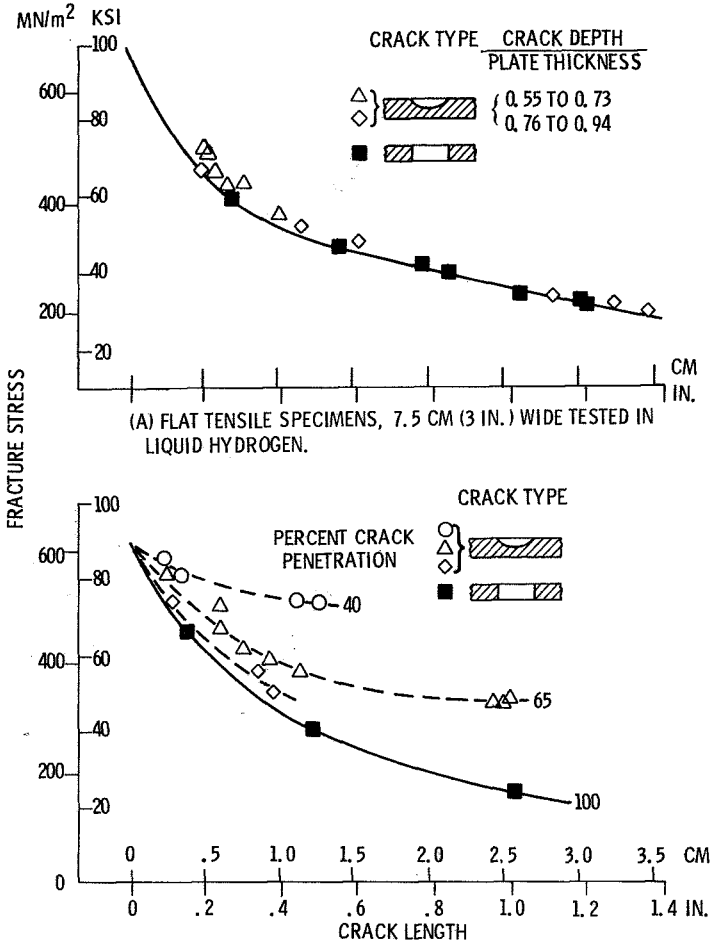

Figure 30. - Fracture strength for 2014-16 aluminum with surface cracks or through-thickness cracks. Nominal thickness, 1.5 mm (0.06 in.).

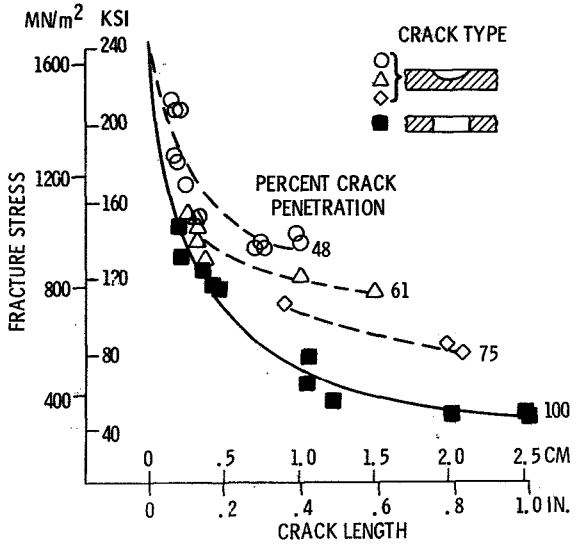

Figure 31. - Fracture strength for Ti-5Al-2.5Sn-ELI tensile specimens with surface cracks or through-thickness cracks. Nominal thickness, 1.5 mm (0.06 in.); specimen widths 2.5, 5.0, and 7.5 cm (1, 2, and 3 in.). Tested in liquid hydrogen.

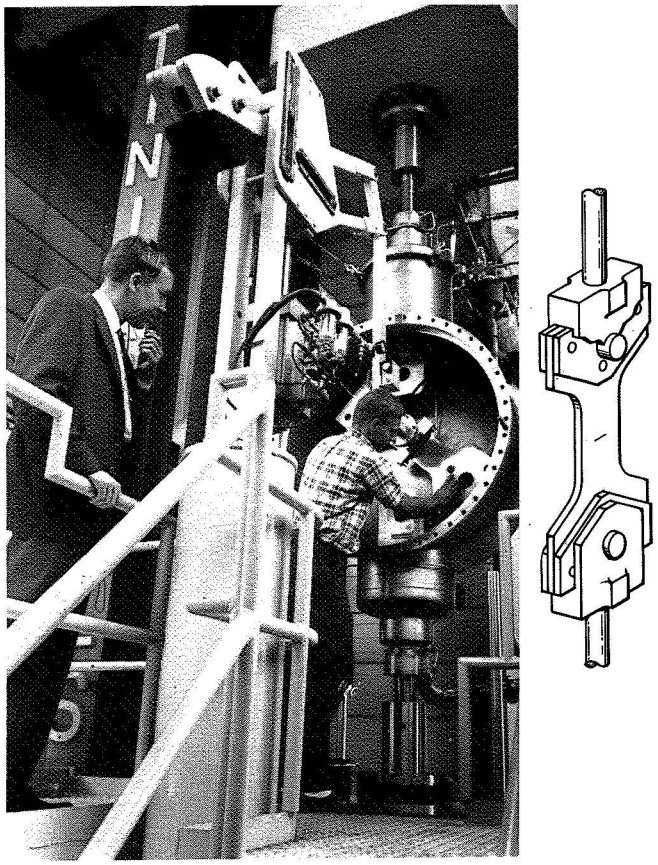

Figure 32. - View of high-load cryogenic tensile testing facility, showing 5.3-MN (1 200 000-LB)tensile machine, liquid hydrogen cryostat, and (inset) low-heat-capacity loading grips.

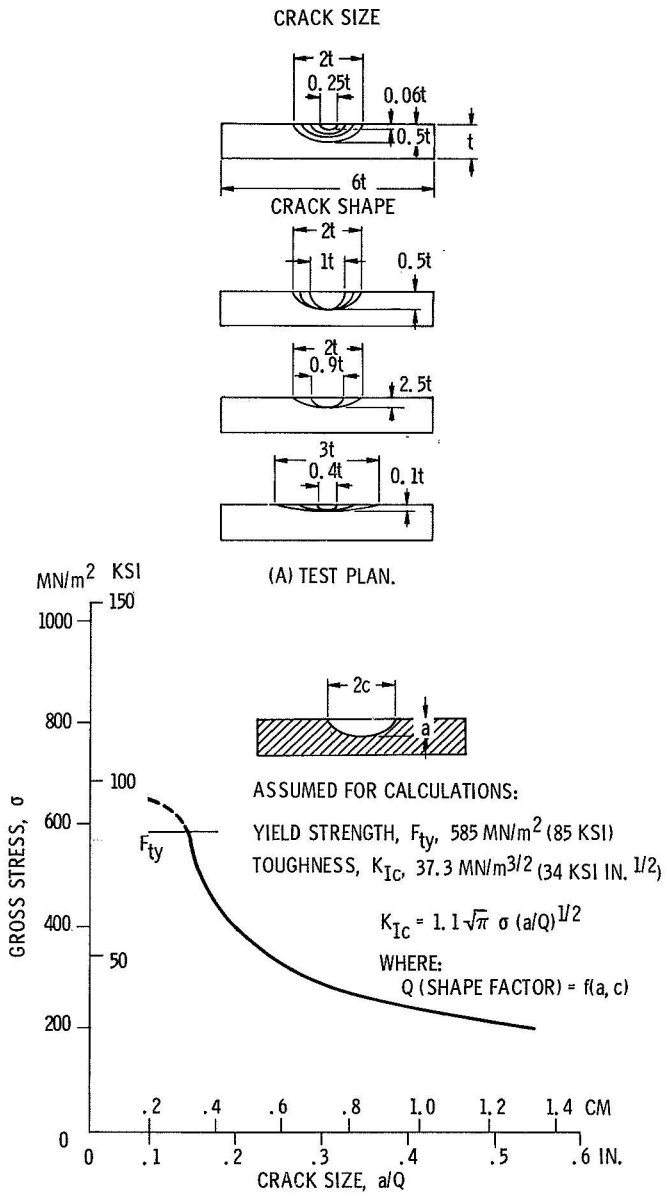

(B) EXPECTED VARIATION OF FRACTURE STRESS WITH CRACK SIZE FOR 2014-T6 ALUMINUM IN LIQUID HYDROGEN.

Figure 33. - Test plan and expected results for surface crack size and shape study.

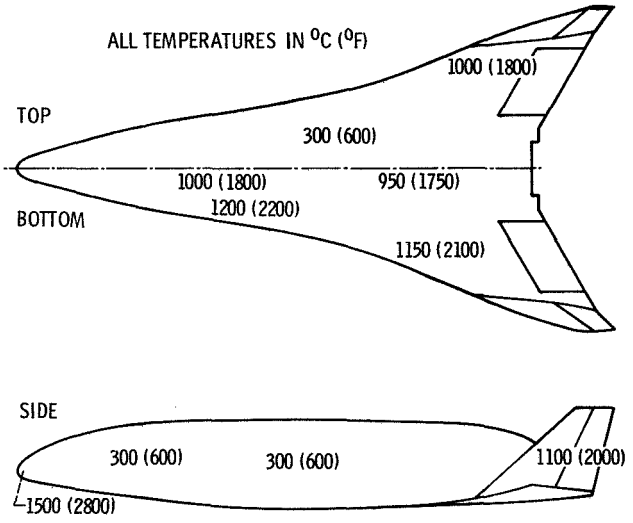

Figure 34. - Approximate temperature distribution for one concept of a space shuttle orbiter.

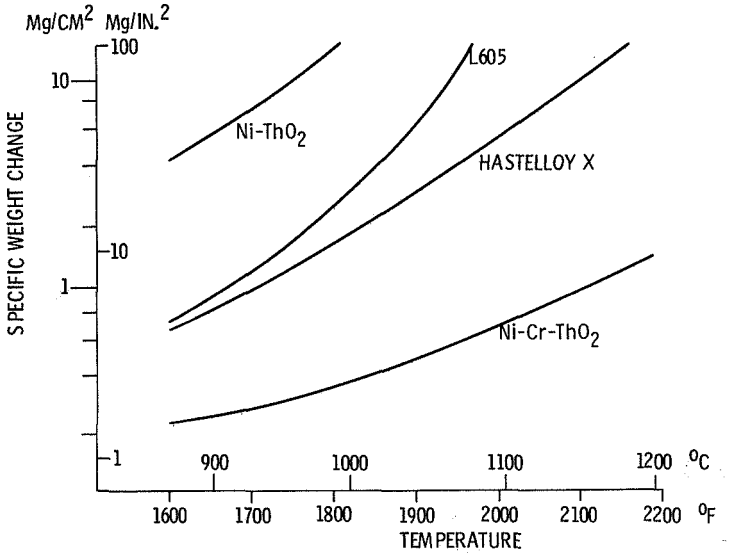

Figure 35. - Oxidation behavior of superalloys in static furnace tests. Samples exposed 600 hours at each temperature.

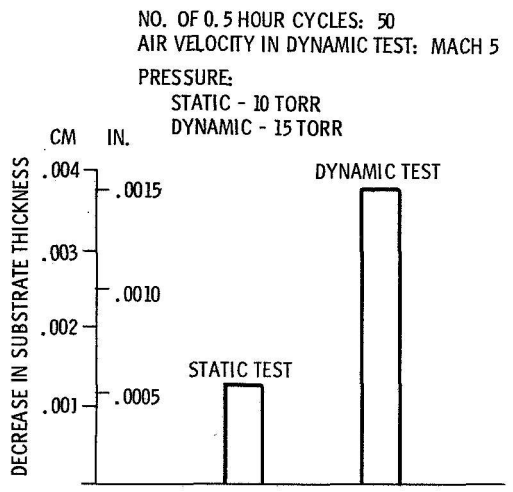

Figure 36. - Comparison of static and dynamic oxidation behavior for TD-NiCr (Ni-20Cr-2 ThO_2) sheet at 1200° C (2200° F).

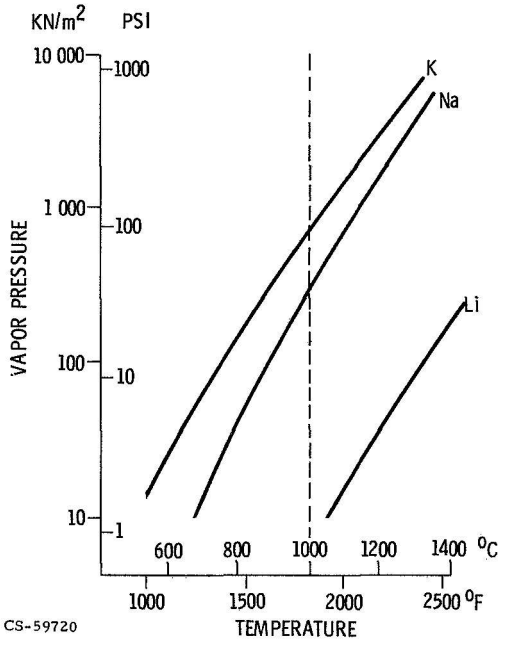

Figure 37. - Effect of temperature on vapor pressure of alkali metals.

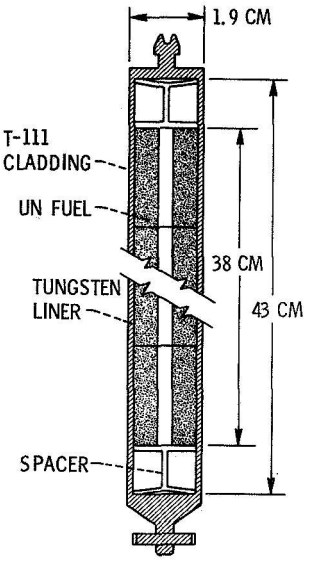

Figure 38. - Space power reactor fuel pin.

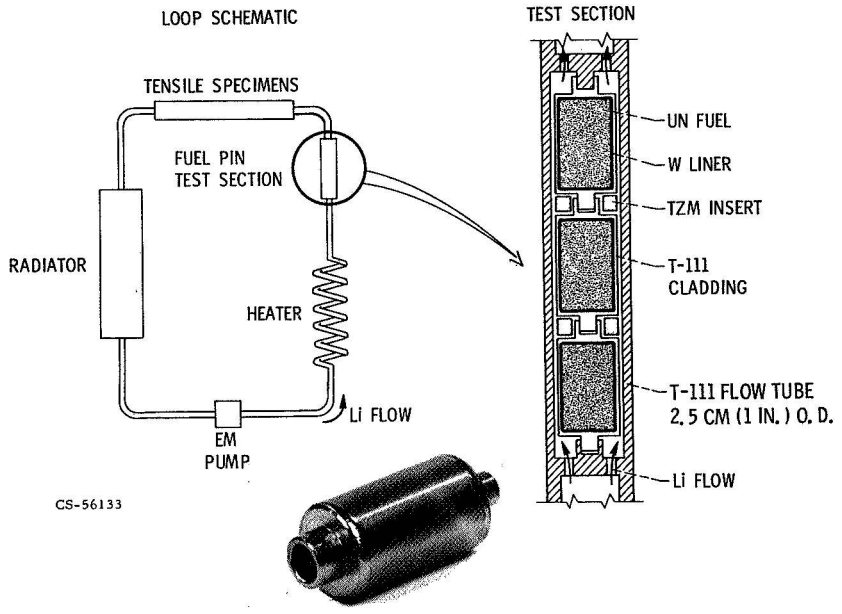

T-111 CLAD UN SPECIMEN AFTER
7500 HOURS IN LOOP

Figure 39. - Pumped lithium loop test, 1040° C (1900° F).

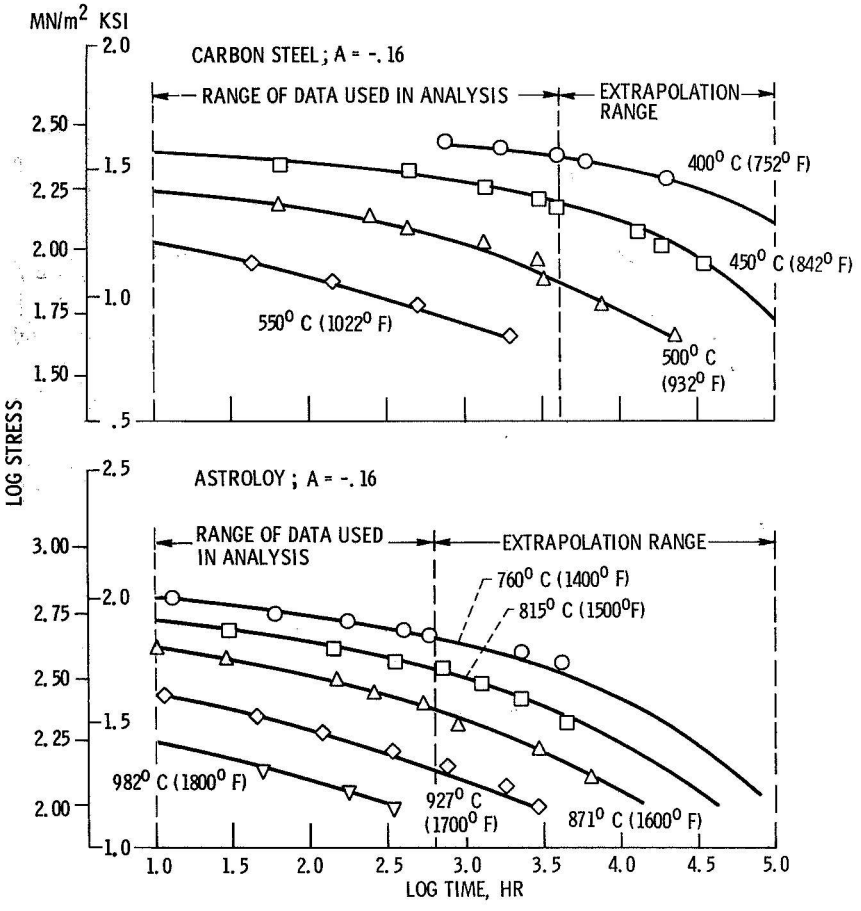

Figure 40. - Extrapolation by parameter log t + AP log t + P.

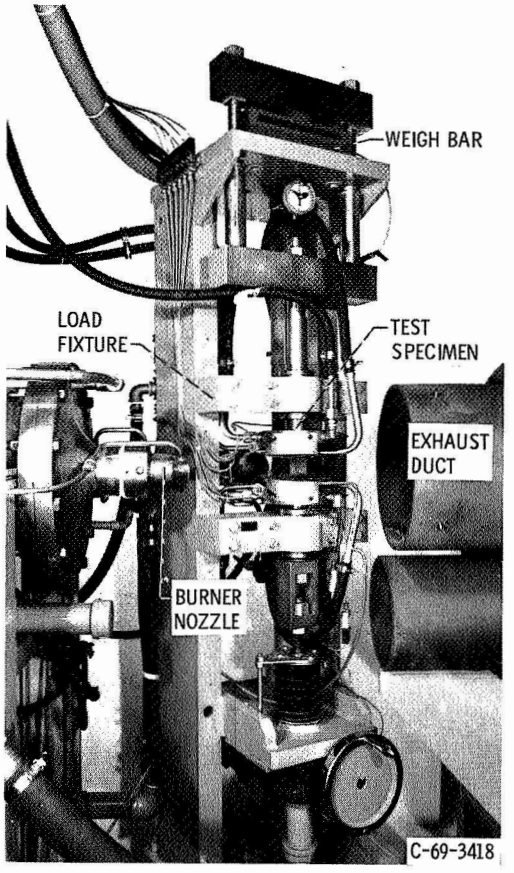

Figure 41. - Apparatus for creep-rupture tests under conditions of high-velocity gas heating.

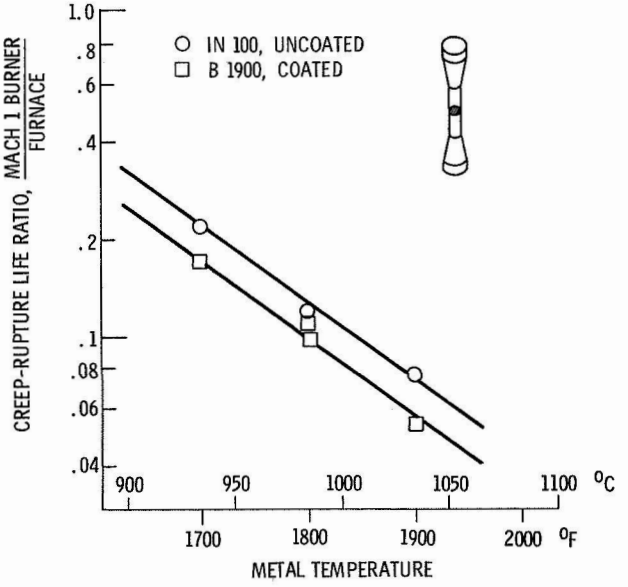

Figure 42. - Effect of gas velocity on creep rupture life.

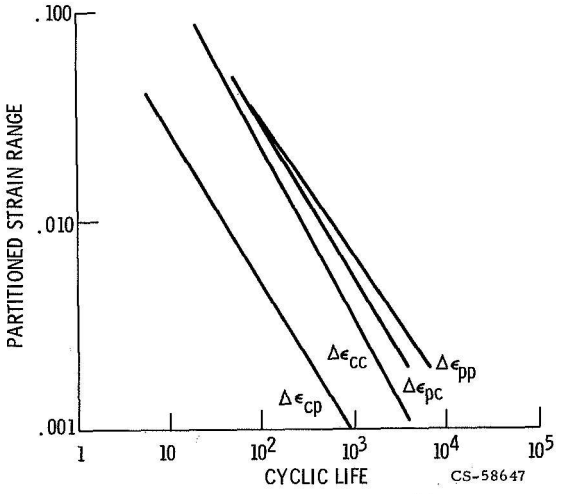

Figure 43. - Partitioned strain range-life relations. Type 316 stainless steel, 705 C (1300° F).

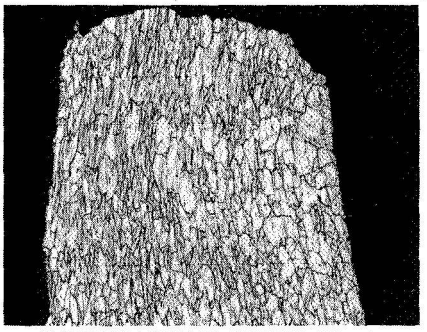

(A) TENSILE PLASTIC FLOW, COMPRESSIVE CREEP. $\Delta\epsilon_{pc}$ = 0.0162, N = 264.

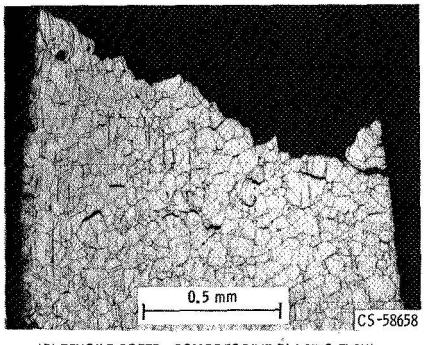

(B) TENSILE CREEP, COMPRESSIVE PLASTIC FLOW. $\Delta\epsilon_{cp}$ = 0.0147, N = 15.

Figure 44. - Photomicrographs of Type 316 stainless steel tested in creep-fatigue. Creep at 705 C (1300 F), plastic flow at 315 C (600 F). Loading direction vertical.

NOTATION	SYMBOL	HYSTERESIS LOOP	DESCRIPTION	
$\Delta\epsilon_{pp}$	○		TENSION PLASTIC COMPRESSION PLASTIC	ISOTHERMAL
$\Delta\epsilon_{pc}$	⌓		TENSION PLASTIC COMPRESSION CREEP	ISOTHERMAL
	△		TENSION PLASTIC COMPRESSION CREEP	PLASTICITY AT LOW TEMPERATURE
	⊐		TENSION PLASTIC COMPRESSION CREEP (RELAXATION)	ISOTHERMAL
$\Delta\epsilon_{cp}$	⌔		TENSION CREEP COMPRESSION PLASTIC	ISOTHERMAL
	▽		TENSION CREEP COMPRESSION PLASTIC	PLASTICITY AT LOW TEMPERATURE
	⊏		TENSION CREEP (RELAXATION) COMPRESSION PLASTIC	ISOTHERMAL
$\Delta\epsilon_{cc}$	□		TENSION CREEP COMPRESSION CREEP	ISOTHERMAL
	▱		TENSION CREEP (RELAXATION) COMPRESSION CREEP (RELAXATION)	ISOTHERMAL

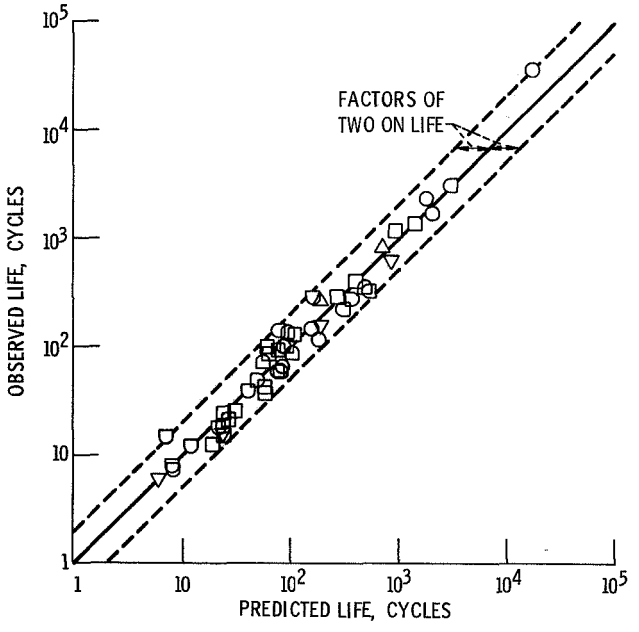

Figure 45. - Summary of life predictability by strain range partitioning. Type 316 stainless steel, 705 C (1300 F).

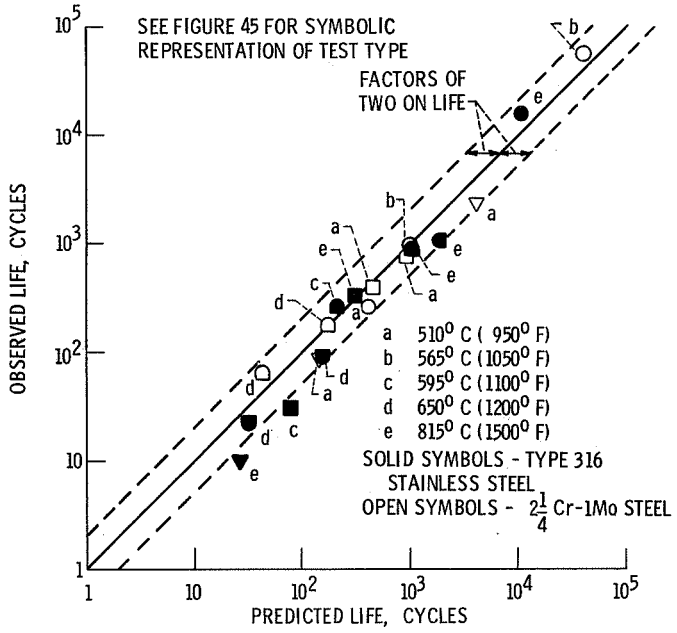

Figure 46. - Applicability of strain range partitioning approach to broad range of temperatures.